

Collagen/hyaluronan based hydrogels releasing sulfated hyaluronan improve dermal wound healing in diabetic mice via reducing inflammatory macrophage activity

Sophia Hauck^a, Paula Zager^a, Norbert Halfter^b, Elke Wandel^a, Marta Torregrossa^a, Ainur Kakpenova^a, Sandra Rother^{b,1}, Michelle Ordieres^a, Susann Räthel^a, Albrecht Berg^c, Stephanie Möller^c, Matthias Schnabelrauch^c, Jan C. Simon^a, Vera Hintze^b, Sandra Franz^{a,*}

^a Department of Dermatology, Venerology und Allergology, Leipzig University, 04103, Leipzig, Germany

^b Institute of Materials Science, Max Bergmann Center for Biomaterials, Technische Universität Dresden, 01069, Dresden, Germany

^c Biomaterials Department, INNOVENT e.V. Jena, Germany

ARTICLE INFO

Keywords:

4–6)-sulfated hyaluronan
Macrophages
Immunomodulation
Chronic wounds
Hydrogel
Skin inflammation

ABSTRACT

Sustained inflammation associated with dysregulated macrophage activation prevents tissue formation and healing of chronic wounds. Control of inflammation and immune cell functions thus represents a promising approach in the development of advanced therapeutic strategies. Here we describe immunomodulatory hyaluronan/collagen (HA-AC/coll)-based hydrogels containing high-sulfated hyaluronan (sHA) as immunoregulatory component for the modulation of inflammatory macrophage activities in disturbed wound healing. Solute sHA downregulates inflammatory activities of bone marrow-derived and tissue-resident macrophages *in vitro*. This further affects macrophage-mediated pro-inflammatory activation of skin cells as shown in skin *ex-vivo* cultures. In a mouse model of acute skin inflammation, intradermal injection of sHA downregulates the inflammatory processes in the skin. This is associated with the promotion of an anti-inflammatory gene signature in skin macrophages indicating a shift of their activation profile. For *in vivo* translation, we designed HA-AC/coll hydrogels allowing delivery of sHA into wounds over a period of at least one week. Their immunoregulatory capacity was analyzed in a translational experimental approach in skin wounds of diabetic db/db mice, an established model for disturbed wound healing. The sHA-releasing hydrogels improved defective tissue repair with reduced inflammation, augmented pro-regenerative macrophage activation, increased vascularization, and accelerated new tissue formation and wound closure.

1. Introduction

Non-healing chronic wounds of the skin represent a significant health problem with increasing incidence due to demographic change and the association of chronic wounds with comorbidities such as obesity, diabetes and vascular diseases that also increase worldwide [1]. Although various therapies are available for treatment and care of chronic wounds, their effectiveness is usually limited and relapse occur in a large number of the patients [1,2]. Increasing case numbers and poor treatment outcomes demand for the development of new, more

effective therapeutic approaches.

Chronic wounds are characterized by a persistent inflammation that leads to excessive tissue breakdown and prevents the injured skin tissue from healing [3]. The unrestrained inflammatory loop therefore represents a promising target in the development of new therapeutic strategies [4,5]. Macrophages play a key role in controlling dermal wound healing and are actively involved in restoring tissue homeostasis after a skin injury [6]. For this, they polarize into different activation states with pro-inflammatory functions or pro-regenerative and anti-inflammatory functions, which are classically assigned to M1-or M2-like macrophage phenotypes, respectively [7]. In chronic wounds,

Peer review under responsibility of KeAi Communications Co., Ltd.

* Corresponding author. University Leipzig, Department of Dermatology, Venerology and Allergology, Max Bürger Research Centre, Johannisallee 30, 04103, Leipzig, Germany.

E-mail address: sandra.franz@medizin.uni-leipzig.de (S. Franz).

¹ Current Address: Department of Cellular and Molecular Medicine, University of California, San Diego, La Jolla, CA, USA

<https://doi.org/10.1016/j.bioactmat.2021.04.026>

Received 15 December 2020; Received in revised form 14 April 2021; Accepted 15 April 2021

2452-199X/© 2021 The Authors. Publishing services by Elsevier B.V. on behalf of KeAi Communications Co. Ltd. This is an open access article under the CC

BY-NC-ND license (<http://creativecommons.org/licenses/by-nc-nd/4.0/>).

Abbreviations

aECM	artificial extracellular matrix
aSMA	alpha smooth muscle actin
BM	bone marrow
ECM	extracellular matrix
GAG	glycosaminoglycan
HA	hyaluronan
HA-AC	acrylated hyaluronan
HYAL	hyaluronidase
IF	immunofluorescence
LPS	lipopolysaccharide
MMP	matrix metalloproteinase

MSC	mesenchymal stromal cells
NFkB	nuclear factor 'kappa-light-chain-enhancer' of activated B-cells
NLRP3	nod-like receptor protein 3
PA	palmitic acid
PBS	phosphate buffered saline
PMN	polymorphonuclear neutrophils
RELMa	resistin-like molecule alpha
sHA	high-sulfated hyaluronan
STAT1	signal transducer and activator of transcription 1
TGF- β 1	transforming growth factor-beta 1
TLR	toll-like receptor
VEGF	vascular endothelial growth factor

the sequential polarization of macrophages in M1 and M2 is disturbed and M1-macrophage activities persist [8,9]. The resulting pro-inflammatory environment hamper the activation of M2-macrophage functions that are crucial for inflammatory resolution and new tissue formation [10,11]. Therefore, reversal of inflammation and restoration of M2 macrophage polarization is hypothesized to be a promising means in treating non-healing wounds [12]. Indeed, redirecting macrophage activities in wound tissue, e.g. by blocking factors that drive inflammation, like IL-1b, TNF or ROS or by application of immunomodulatory cells such as mesenchymal stromal cells (MSCs) or fibroblasts that promote M2 macrophage polarization, was shown to improve impaired wound healing [9,13–18]. Despite these promising observations, implementation of controlling macrophage functions in chronic skin wounds by an applicable immunomodulating wound dressing is still lacking.

Within the recent years, regenerative medicine research has focused on the development of biologic active materials for a variety of clinical applications that interact with and modulate the wound environment to promote functional tissue remodeling and to induce favorable healing outcomes [19,20]. In this respect, the extracellular matrix (ECM) has been recognized as an important regulator of cell differentiation and activation. Thus, most of these materials are composed of naturally-derived ECM or synthetic ECM components to mimic specific physiological cell-instructive abilities of the ECM [21,22].

Glycosaminoglycans (GAG) are components of the extracellular matrix (ECM) that control cell functions either directly via receptor binding and signaling or indirectly via processing the availability and bioactivity of growth factors and cytokines that signal to the cells [23]. Particularly the non-sulfated GAG hyaluronan (HA) possesses potent anti-inflammatory properties and downregulates pro-inflammatory activities of immune cells including macrophages via direct receptor-mediated interaction with the cells [24–27]. However, immunoregulatory activity of HA is controlled by its molecular size with high molecular weight HA promoting inflammatory resolution while its degradation to small fragments favors progression of inflammation [28, 29].

We have recently shown that immunoregulatory activities of HA can be refined, enhanced and uncoupled from its molecular size by chemical modification with sulfate groups. Particularly HA derivatives with a high degree of sulfation exert a strong anti-inflammatory effect on human macrophages in culture *in vitro* and promote the activation of regulatory functions independent of its molecular weight and superior to large HA polymers [30]. We also demonstrated that 2-dimensional artificial ECM composed of collagen as a protein network and incorporated with high-sulfated HA (sHA) that leaks from the matrix modulate monocyte to macrophage differentiation in inflammatory conditions and promote the activation of regulatory macrophage functions [31,32]. This suggests sHA as a promising immunoregulatory component for the design of a functional wound dressing biomaterial to control

macrophage activities at sites of non-healing wounds. This concept was explored in this study.

We investigated the capability of sHA to modulate functions of tissue-resident and bone marrow-derived macrophages in *in vitro* settings mimicking the pro-inflammatory and pathological environment of chronic wounds. Using a skin *ex vivo* culture model, we examined consequences of this regulation on the macrophage-mediated activation of skin cells. We further investigated the immunomodulatory effect of sHA in a mouse model of acute skin inflammation where we analyzed its capacity to prevent and to rescue inflammation. Finally, we designed hyaluronan/collagen (HA/coll)-based hydrogels allowing a continuous release of sHA and assessed the capability of these hydrogels to control inflammation and macrophage activities in skin wounds of db/db mice, an established model for delayed diabetic wound healing.

2. Material & methods

2.1. HA derivative, artificial extracellular matrix and hydrogel preparation

Biotechnologically produced HA from Streptococcus (Aqua Biochem, Germany) with molecular weight of 1,100,000 g mol⁻¹ (H-HA) was thermally degraded in a controlled manner and used for acrylation (HA-AC) and sulfation (sHA) of HA as described previously [33–36]. Table 1 summarizes the results of the chemical characterization of the synthesized HA derivatives, which was performed as reported in Refs. [33,36]. In the preparation of high-sulfated HA the average number of sulfate groups per repeating HA disaccharide unit (D.S._S) can vary slightly from batch to batch between 2.8 and 3.4. In this study, four different high-sulfated HA batches were used, which had D.S._S values of 3.0, 3.1, 3.2 and 3.4, respectively, and which are summarized in Table 1 with D.S._S 3.0–3.4. In comparative experiments we confirmed that the different batches showed no differences in their effect on macrophages and inflammation processes (data not shown).

An artificial extracellular matrix (aECM) suspension consisting of either collagen only or collagen/sHA was obtained by *in vitro* fibrillogenesis at 37 °C after mixing 3 mg/ml collagen type I (rat tail, Corning,

Table 1

Characteristics of HA derivatives. ¹D.S._S: Average number of sulfate groups per repeating HA disaccharide unit; ²D.S._{AC}: Average number of acrylate groups per repeating HA disaccharide unit; ³Mw: Weight-average molecular weight determined by gel permeation chromatography (GPC) with laser light scattering (LLS) detection.

Sample	L-HA	HA-AC	sHA
D.S. _S ¹	-	-	3.0–3.4
D.S. _{AC} ²	-	0.16	-
Mw (kDa) ³	48.3–48.8	106.8	47.5–52.8

Germany) dissolved in 10 mM acetic acid with fibrillogenesis buffer (10 mM KH_2PO_4 and 50 mM Na_2HPO_4 , pH 7.4) with or without 7.5 mM (6 mg/ml) disaccharide units of sHA.

HA-AC-based hydrogels were prepared according to Refs. [37,38]. In brief, HA-AC was dissolved in aECM suspension to a final HA-AC concentration of 50 mg/ml. Afterwards, 10 mg/ml photo initiator lithium phenyl-2,4,6-trimethyl-benzoylphosphinate (LAP, TCI Deutschland GmbH, Germany) was mixed with the HA-AC/aECM suspensions in a 1:10 ratio. Thin hydrogels with sHA (HA-AC/coll/sHA) or without (HA-AC/coll) were prepared from 45 μl polymer solution, which was pipetted between two glass slides (12 mm diameter) prior to UV light irradiation (365 nm, 0.17 W/cm²) and lyophilization (Suppl. Fig.1).

The collagen and sHA distribution within the hydrogels were visualized using Sirius red and Toluidine blue. The stability and release behavior were analyzed after hydrogel incubation in phosphate buffered saline (PBS, pH 7.4) for up to 8 days by quantifying the amounts of released collagen, HA-AC and sHA in the supernatants using the Lowry method, turbidity measurements via HA-AC/cetyltrimethylammonium bromide complexes and the 1,9-dimethylmethylene blue (DMMB) assay [39–42]. The remaining amounts of collagen, HA-AC and sHA were calculated from the difference between the original amount and the detected quantities in the supernatants using the respective standards as described previously [36,37].

2.2. Hydrogel morphology

After lyophilization of the hydrogels, the scaffolds were cut in halves and mounted to stubs following sputter coating with a thin carbon layer (Baltec, Germany). The morphology was assessed by scanning electron microscopy (SEM, Philips ESEM XL 30, FEI) using the secondary electron detector.

2.3. Elastic modulus of hydrogels

Hydrogels were produced as described in 2.1 but 40 μl and cylindrical mold casts ($\varnothing = 4$ mm, $h = 3.1$ mm) were used instead. After lyophilization swelling in PBS for 1 h followed. Force-displacement curves were measured with a CellScale MicroTester (Waterloo, Canada) using 10% displacement during a loading phase of 2 min. The elastic moduli were determined from the linear area of the stress-strain curves.

2.4. Enzymatic in vitro hydrogel degradation

Hydrogels were incubated in 600 μl either 10 mM acetic acid pH 5.35 or PBS pH 7.4 containing 1000 U/ml hyaluronidase (HYAL, EC 3.2.1.35, from bovine testes) at 37 °C for up to 7 d. 200 μl supernatants were collected at different time points and replaced by 200 μl freshly prepared HYAL solution. The total amount of GAG degradation products in the supernatants was determined using the hexosamine assay [43,44]. The amount of sHA in the supernatant was determined with the 1,9-dimethylmethylene blue (DMMB) assay [41]. The amount of GAG remaining in the hydrogels was calculated with respect to the initial amount of GAG in the hydrogels.

2.5. Generation and culture of tissue-resident and bone marrow-derived macrophages

Macrophages were generated from peritoneal lavage cells or from bone marrow (BM) aspirates from hindlimbs of C57BL/6 mice as described [45,46]. Briefly, for peritoneal cells, the peritoneum of a mouse was lavaged with 2 ml PBS using a 21-G needle. For bone marrow leukocytes, bone marrow was flushed out of trimmed leg bones using RPMI 1640 medium (ThermoScientific, Karlsruhe, Germany) and a 25-G needle. Red blood cells were lysed before cell culture. Peritoneal cells were cultured at 4×10^5 cells/ml in RPMI 1640 medium

(ThermoScientific) containing 10% fetal calf serum (FCS, ThermoScientific), 1% penicillin/streptomycin (Biochrom GmbH, Berlin, Germany), and 5 ng/ml M-CSF (Miltenyi, Bergisch-Gladbach, Germany) for 24 h to generate tissue-resident peritoneal macrophages (pMa). Bone-marrow cells were cultured at 2×10^6 cells/ml in RPMI plus 10% FCS, 1% P/S and 5 ng/ml M-CSF for 7 days to generate BM-derived macrophages (BM-Ma). Before stimulation BM-Ma were harvested and seeded at 4×10^5 cells/ml per well.

Differentiated macrophages were stimulated as follows: BM-Ma and pMa were co-stimulated with 100 ng/ml LPS (Sigma) and either 500 $\mu\text{g}/\text{ml}$ sulfated hyaluronan (sHA), high molecular weight HA (H-HA) or low molecular weight HA (L-HA), respectively. As control non-stimulated and LPS-stimulated pMa and BM-Ma were cultured in the absence of HA derivatives. Peritoneal cells were cultured with or without 500 $\mu\text{g}/\text{ml}$ sHA. After 24 h 500 μM PA (Sigma-Aldrich) complexed to bovine serum albumin (BSA) or BSA was added 5 h prior to stimulation with 100 ng/ml LPS as previously described [45]. As controls pMa were cultured with PA or BSA without sHA and LPS. Cells were analyzed 24 h after LPS stimulation. To prepare supernatants for skin *ex-vivo* culture, peritoneal cells were cultured in the presence or absence of sHA for 24 h. Cells were washed and stimulated with LPS for further 24 h. Unstimulated peritoneal cells were cultured as control.

2.6. Ex-vivo skin culture

Skin biopsies (6 mm) generated from C57BL/6 mice were cultured in supernatants from peritoneal cells as described above. Skin samples were harvested after 24 h and prepared for isolation of epidermal cells.

2.7. Animal studies

All animal experiments were performed according to institutional and state guidelines and were approved by the Committee on Animal Welfare of Saxony (Germany, TVV19/12, TVV24/12, TVV33/17, TVV25/19).

2.8. Imiquimod-induced skin inflammation

Skin inflammation was induced in 8–10 weeks old BALB/c mice by topical application of Aldara creme containing 5% imiquimod (IMQ) (Meda GmbH, Wiesbaden, Germany) on the shaved back. In the prevention approach, 50 mg Aldara was applied on three consecutive days. Immediately before each IMQ treatment 500 μg HA derivatives (H-HA, L-HA or sHA, respectively) dissolved in 100 μl PBS or 100 μl PBS (control) were injected in the skin. Lesional skin was analyzed at day 3 and day 4. In the therapy approach, one dose Aldara (125 mg) was applied and either 500 μg sHA or 100 μl PBS were injected in the skin after one day. Lesional skin was analyzed at day 3. Erythema and scaling were documented photographically. Skin was embedded in tissue freezing medium (Leica) for histological analyses (HE and immunofluorescence (IF) staining with Ki67 and CD11b) of tissue sections. Cell suspensions from the skin were prepared for immune cell analysis by flow cytometry and magnetic cell separation of CD11b + immune cells from the skin. In addition, RNA was isolated from skin for gene expression analysis.

2.9. Wound healing

Wound healing studies were performed in 10–12 weeks old diabetic db/db mice as previously described [4]. Full-thickness wounds (including panniculus carnosus) were inflicted with 6-mm dermal biopsy punches on both sites of the shaved back. At day three after wounding hydrogel discs (12 mm) were applied to the wounds and covered with Mepitel (Mölnlycke Health Care) and Raucodrape (Lohmann & Rauscher) to keep the materials in place and moisturized. Wounds were analyzed 10 days after wounding. Wounds were photographed prior to excision from the skin. Wounds were deep-frozen in

tissue freezing medium for HE and IF (CD31, aSMA, panCK, Ki67, RELMa and F4/80) staining of wound sections. Wounds were further prepared for tissue lysis to isolate RNA for gene expression analysis or to quantify cytokines by ELISA.

2.10. Preparation of cell suspension and isolation of cells from lesional skin

Epidermal cells were isolated from cultured skin upon segregation of the epidermis from dermis after incubation with 0.25% trypsin (Biotech, Berlin, Germany) overnight. Cell suspension was prepared from lesional skin by enzymatic digestion of skin with 0.25 mg/ml liberase (Roche, Mannheim, Germany) in the presence of 0.06 mg/ml DNase (Sigma-Aldrich Chemie GmbH, Taufkirchen, Germany) for 1 h as described [45]. Myeloid cells were isolated using CD11b MicroBeads (Miltenyi, BergischGladbach, Germany) according to manufacturer's instructions. Isolated epidermal cells and myeloid cells were immediately prepared for RNA preparation.

2.11. RNA preparation and quantitative real-time PCR

Total RNA from homogenized lesional skin, wound tissue, cells isolated from lesional skin, cultured macrophages and epidermal cells was isolated either with ReliaPrep RNA Tissue Miniprep System (Promega, Walldorf, Germany) or with RNeasy Mini Kit (Qiagen) according to the manufacturer's protocol. At least 0.15 µg RNA was used for first-strand cDNA synthesis with either Thermo Scientific RevertAid Reverse Transcriptase (Thermo Fisher Scientific) or LunaScript RT SuperMix Kit (New England Biolabs, Frankfurt a.M., Germany) according to the

manufacturer's protocol. Quantitative real-time qPCR was performed with intercalating dye technology (GoTaq qPCR Master Mix (Promega) or Luna Universal qPCR Master Mix (New England Biolabs)) according to the manufacturer's instructions. Primer sequences are listed in Table 2. Quantitative gene expression was calculated using a simultaneously recorded standard curve of cloned cDNA, normalized to the unregulated reference genes RS36B4 or GAPDH and computed as arbitrary units of mRNA.

2.12. Protein isolation from wound lysates

Wound tissue was cut into small pieces and transferred in cell lysis buffer (BD) containing 1 mM phenylmethylsulfonyl fluoride, followed by mechanical disruption at 25 Hz for 6 min using a 5-mm steel bead and a bead mill (TissueLyser LT, Qiagen). Tissue debris was removed from the protein suspension by centrifugation for 10 min. Wound lysates were used for cytokine determination by ELISA.

2.13. ELISA

Cytokines were assessed in cell-free supernatants of peritoneal cells or in wound lysates. The following murine cytokines were quantified by ELISA according to the manufacturer's instructions and detected using Synergy HT (BioTek, Bad Friedrichshall, Germany): IL-1β, TNF, IL-6, IL-10 and CCL2 (ELISA MAX Standard Sets, BioLegend).

2.14. Flow cytometry

Cell suspension from lesional skin was incubated with antibody

Table 2
Primer sequences and annealing temperatures (T_{anneal}) used for qPCR.

Gene		Sequence (5' → 3')	T_{anneal}	Accession number
IL-1b	Fwd	GACAACCTGCACTACAGGCTCC	60 °C	NM_008361.3
	Rev	AGGCCACAGGTATTTGTGCG		
TNFa	Fwd	CTTAGACTTTGCGGAGTCCG	62 °C	NM_013693.3
	Rev	ACAGTCCAGGTCACCTGTC		
CXCL1	Fwd	CAGTGCCTGCAGACCATG	62 °C	NM_008176.3
	Rev	CTGAACCAAGGAGCTTACAG		
IL6	Fwd	GCCTATTGAAAATTCCTCTGG	60 °C	NM_031168
	Rev	AAGATGAATTGGATGGTCTTGG		
CCL2	Fwd	TCAGCCAGATGCAGTTAAG	61 °C	NM_011333.3
	Rev	TCTGGACCCATTCTCTCTG		
S100A8	Fwd	ACTGAGTGTCTCAGTTGTGC	58 °C	NM_013650
	Rev	CCCTAGGCCAGAAGCTCTG		
S100A9	Fwd	ACTCTAGGAAGGAAGGACACCC	58 °C	NM_009114
	Rev	TACACTCTCAAAGCTCAGCTG		
IL-1RA	Fwd	GACCCCTGCAAGATGCAAGCC	64 °C	NM_031167.5
	Rev	CAGGACGGTCAAGCTCTAGT		
CCR2	Fwd	GCAGGTGACAGAGACTCTTGG	61 °C	NM_009915.2
	Rev	CTCACTCGATCTGCTGTCTCC		
IL-10	Fwd	AGCCGGGAAGACAATAACTG	61 °C	NM_010548.2
	Rev	CATTTCGGATAAGGCTTGG		
F4/80	Fwd	TCACTGTCTGCTCAACCGTC	58 °C	NM_010130.4
	Rev	TGCCATCAACTCATGATACCCCT		
HO-1	Fwd	GACACTGAGGTCAAGCACAG	65 °C	NM_010442.2
	Rev	CCACTGCCACTGTGGCCAAAC		
Relma	Fwd	CCCTCCACTGTAACGAAGAC	61 °C	NM_020509.3
	Rev	CAACGAGTAAGCACAGGCAG		
EGF	Fwd	TCACTGGACAGCTACACATGC	62 °C	NM_010113.4
	Rev	CCACATCCCCAAGACGAG		
Ki67	Fwd	GATGCAAAAACCTTGAAGGAGG	58 °C	NM_001081117.2
	Rev	GGAGGTGAAAACCACTGG		
CD31	Fwd	TCACCAAGAGAACGGGAAGGC	58 °C	NM_001032378.2
	Rev	CTGGAACCTCCTTTCACCCC		
VEGF	Fwd	AGGATGTCTCACTCGGATG	60 °C	NM_001025250.3
	Rev	CTGTCTCTTGACTCAGGGC		
RS36B4	Fwd	GGACCCGAGAAGACCTCCTT	62 °C	NM_007475
	Rev	GCACATCACTCAGAATTCAATGG		
GAPDH	Fwd	TGGCAAAGTGGAGATTGTGCC	55 °C	NM_008084
	Rev	AAGATGGTGATGGGCTTCCC		

mixture including anti-F4/80-PE (BioRad, Munich, Germany), anti-Ly6G-FITC, anti-CD11b-PECy7, anti-CD45-PerCPy5.5 and anti-Ly6C-APC (all Biolegend) for 30 min at 4 °C. After washing, cells were stained with Zombie NIR™ (Biolegend) to label dead cells and immediately analyzed. Flow cytometry was performed with BD FACS Canto II (BD Biosciences, Heidelberg, Germany) and data analyzed using BD FACSDIVATM software (BD Biosciences). Cells were gated as described [14]. In brief, single cells were selected and dead cells excluded via positive stain for Zombie NIR™. Within the population of viable cells, co-expression of CD45 and CD11b was used to mark immune cells. Within the population of CD45+/CD11b+ cells PMN are defined by expression of Ly6G. Cells negative for Ly6G are further defined as monocytes/macrophages (Mo/Ma) due to their Ly6C and F4/80 expression.

2.15. Histology (H&E) and immunostaining of cryo-sections

Cryo-sections of lesional skin and wounds were stained with hematoxylin and eosin staining (H&E) using standard protocols. For immunostaining cryo-sections were fixed in acetone for 10 min, washed with PBS and blocked with 1% goat serum (Sigma) in PBS for 1 h before staining with primary antibodies overnight in antibody diluent buffer (Dako). Primary antibodies used and dilutions were: anti-mouse CD11b-PE (Miltenyi, clone M1/70.15.11.5) 1:50, rat anti-mouse F4/80 (AbD Serotec, clone A3-1) 1:200, rat anti-mouse CD31 (Dianova, clone SZ31) 1:100, anti-mouse pan-cytokeratin (panCK)-FITC (Sigma, clones C-11+PCK-26+CY-90+KS-1A3+M20+A53-B/A2) 1:100, anti-mouse α SMA-Cy3 (Sigma, clone 1A4) 1:200, rabbit anti-mouse Ki67 (Bethyl Laboratories, polyclonal) 1:400, rabbit anti-mouse RELMa (Peprotech, polyclonal) 1:50. Primary antibody binding of F4/80, CD31, Ki67, RELMa was detected by incubation with either of the following secondary antibodies: goat anti-rat Alexa Fluor 594 (Invitrogen, 1:1000), goat anti-rabbit Alexa Fluor 546 (Life Technologies, 1:1000), goat anti-rat Alexa Fluor 488 (Invitrogen, 1:1000), goat anti-rabbit Cy5 (JacksonImmunoResearch, 1:400). Counterstaining with DAPI 1:500 (Invitrogen) was used to visualize cell nuclei. Morphometric analysis was performed on hematoxylin/eosin (H&E)-stained tissue cryo-sections using light microscopy. Microscopy of immunostainings was performed with a Keyence BZ-9000 microscope (Biorevo) equipped with fluorescence and image capturing system. Wound closure was evaluated in panCK immunostainings. Wounds completely covered with neopithelium were defined as closed. Count of Ki67-positive cells, CD11b-positive cells, F4/80-positive cells and area of CD31 positive tissue and of F4/80 and RELMa co-localization in tissue sections of lesional skin and wound tissue sections, respectively, were quantified using the Keyence BZ-9000 software (Biorevo).

2.16. Statistics

All *in vitro* experiments were performed with cells and skin samples from at least four or more different mice. Data are presented as means \pm SD. For statistical analyses GraphPad Prism7 (GraphPad Software, Inc., San Diego, CA, USA) was used. Data analysis was performed using paired or unpaired student t-test or using one-way ANOVA or two-way ANOVA with multiple comparisons versus indicated control. Any P values < 0.05 were considered to be statistically significant. Up to three different degrees of significance were indicated as follows: *P < 0.05; **P < 0.01; ***P < 0.001.

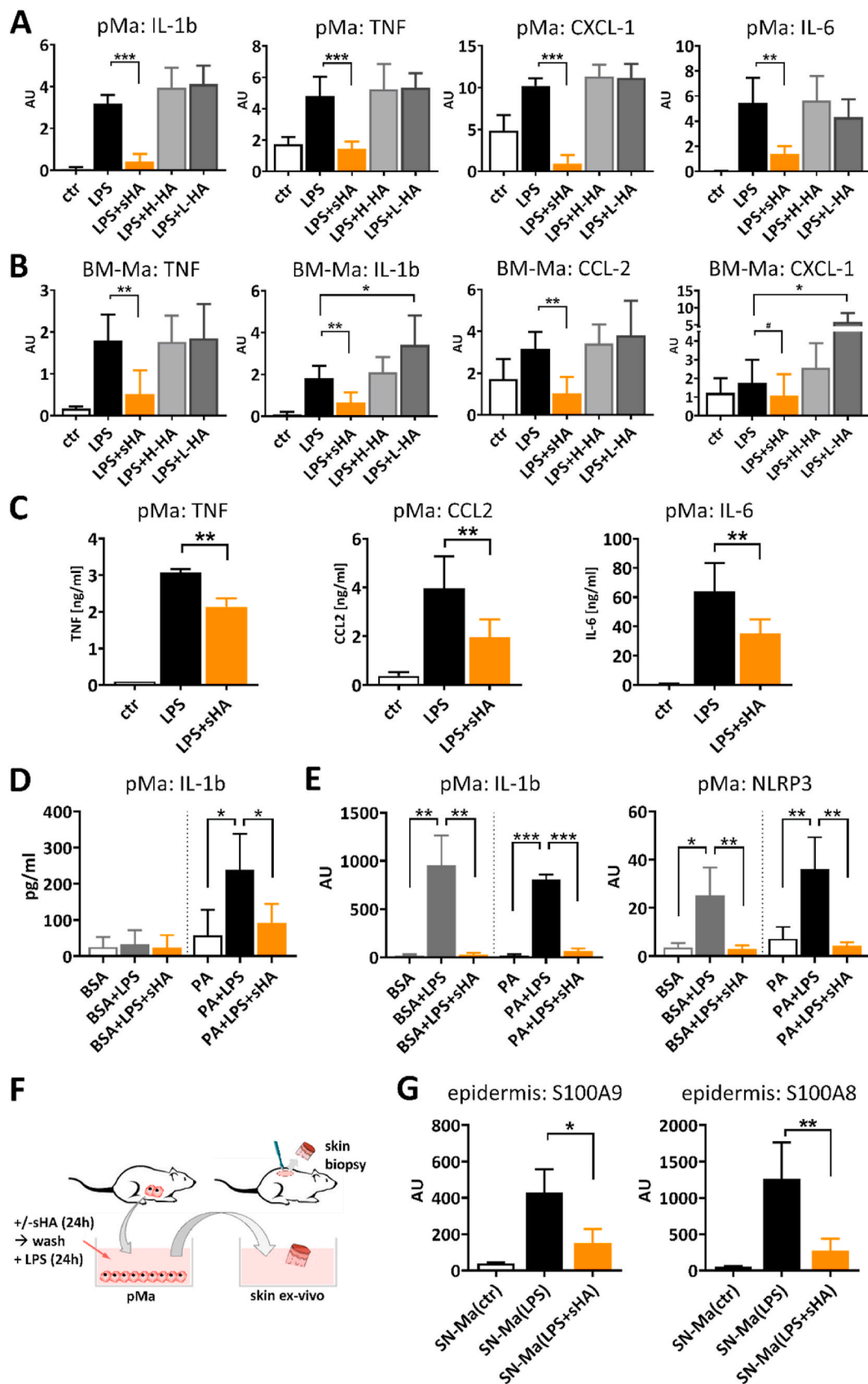
3. Results & discussion

3.1. Sulfated hyaluronan reduces inflammatory function in tissue-resident and bone marrow derived macrophages

Inflammatory responses in the skin and during wound healing involve activities of skin resident macrophages and of macrophages that

differentiate from blood-derived monocytes that infiltrate the wound site [47]. Within a chronic wound environment both resident and infiltrated macrophages undergo a profound inflammatory activation in response to excessive danger signals and toll-like receptor (TLR) activation and pro-inflammatory cytokine signaling in the tissue [48]. To assess whether sHA has the potential to regulate both types of macrophages in the tissue, we first investigated the impact of sHA on peritoneal cells as a source of resident macrophages [49] and on bone marrow (BM-) derived macrophages. Peritoneal cells and BM-macrophages were generated from healthy wild-type mice and cultured in the presence of high-sulfated HA (sHA), high molecular weight HA (H-HA) serving as an anti-inflammatory positive control or low molecular weight HA (L-HA) of the same molecular size as sHA and thus serving as size control. All cells were stimulated with the TLR agonist LPS to mimic a pro-inflammatory activation as it occurs in the wound environment. Since our previous studies with human macrophages revealed an intervention of macrophage activation by sHA on transcriptional level and a blockage of the transcription factors NF κ B and STAT-1 [30–32] we analyzed inflammatory gene expression that are controlled by these sHA-targeted transcription factors including IL-1b, TNF, IL-6, CXCL-1 and CCL-2. In both, peritoneal cells and BM-macrophages expression of these genes was significantly downregulated in culture with sHA, while in control settings with H-HA and L-HA gene expression was not altered or in case of BM-macrophage cultures with L-HA partially up-regulated (Fig. 1 A/B). The observed effect of sHA on murine macrophage types confirms findings from other studies showing anti-inflammatory activity of sHA on human macrophages and MSC [30,50]. Contrary to previous findings [27,30], we detected no anti-inflammatory macrophage regulation by H-HA. This difference may arise from the different experimental set-up (24 h culture with HA in this study vs > 48 h culture with HA in other studies) and the different cells that were used (primary murine macrophages in this study vs primary human macrophages or murine macrophage cell lines in Ref. [30] or [27], respectively). However, the fast effect of sHA on the pro-inflammatory macrophage activation highlights the superior immunoregulatory activity of sHA compared to the large HA polymer. Further analyses of the cytokine response showed that blocking inflammatory gene expression by sHA consequently resulted in a reduced release of inflammatory cytokines and chemokines such as TNF, IL-6, CCL2 (Fig. 1C) which is also in line with our previous observations [30,50].

Release of IL-1b involves inflammasome activation that requires the second activating signal for the assembly of the inflammasome complex in addition to a TLR signal like LPS. The latter primes the cell through transcriptional upregulation of effector molecules including IL-1b and inflammasome components like Nod-like receptor protein 3 (NLRP3) [51]. Activation signals include extracellular ATP, pore-forming toxins, RNA viruses and particulate matter [52]. Elevated release of IL-1b by macrophages particularly contributes to pathogenicity in diabetic wound healing [10] and saturated fatty acids (SFA) have been identified to contribute to macrophage inflammasome activation in conditions of obesity and type 2 diabetes [53]. We therefore investigated whether sHA down-regulates IL-1b release from macrophages using SFA as activation signal for required inflammasome activation. We cultured peritoneal cells with the SFA palmitic acid (PA) or BSA (control) in the presence or absence of sHA prior to stimulation with LPS. In line with previous reports [45,54,55], we observed a significant release of high levels of IL-1b in peritoneal cells co-stimulated with LPS and PA in comparison to cells stimulated with PA alone (Fig. 1D). Since free fatty acids circulate in the body as albumin-bound form [56], we applied PA as complex with BSA. We therefore used peritoneal cells cultured in the presence of BSA as control setting. Stimulation of BSA-control cells with LPS alone induced also no release of IL-1b (Fig. 1D) demonstrating that PA provides the second signal for inflammasome activation in the LPS-primed peritoneal cells. Of note, sHA interfered inflammasome activation since release of IL-1b was significantly reduced when sHA was present in the culture of PA-LPS stimulated peritoneal cells (Fig. 1D). In addition, we observed a



(caption on next page)

Fig. 1. sHA down-regulates pro-inflammatory macrophage functions and modulates macrophage crosstalk with skin cells. A-C) Peritoneal cells (pMa) and bone marrow-derived macrophages (BM-Ma) from mice were co-stimulated with LPS and either sulfated hyaluronan (sHA), high molecular weight HA (H-HA) or low molecular weight HA (L-HA), respectively. Non-stimulated (ctr) and LPS-stimulated (LPS) pMa and BM-Ma in the absence of HA derivatives served as control. **A)** Gene expression of pro-inflammatory cytokines IL-1b, TNF, CXCL-1, IL-6 relative to the reference gene RS36B4 in pMa. **B)** Gene expression of pro-inflammatory cytokines IL-1b, TNF, CXCL-1, CCL-2 relative to RPL0 in BM-Ma. **C)** Detection of inflammatory cytokines TNF, IL-6, CCL-2 in pMa culture. **D/E)** pMa were cultured with BSA-complexed palmitic acid (PA) or BSA alone in the presence (BSA+LPS+sHA, PA+LPS+sHA) or absence of sHA (BSA+LPS, PA+LPS) prior to stimulation with LPS. pMa without LPS stimulation (BSA, PA) served as controls. **D)** Detection of released IL-1b in supernatants. **E)** Gene expression of IL-1b, NLRP3 relative to the reference gene GAPDH. **F/G)** Skin biopsy punches from mice were cultured *ex vivo* in supernatants (SN) from LPS-stimulated pMa not pre-treated (SN-Ma(LPS)) or pre-treated with sHA (SN-Ma(LPS + sHA)). Supernatants of unstimulated pMa (SN-Ma(ctr)) served as control. **F)** Schematic illustration of skin *ex vivo* culture experiment. **G)** Gene expression of S100A8 and S100A9 in epidermal layer of cultured skin relative to reference gene RS36B4. Mean \pm standard deviation. $n \geq 4$ independent experiments with cells/skin from different mice. Paired sample analysis: A/B/D/E: One-way ANOVA with multi comparison to LPS or BSA + LPS or PA + LPS; * $p \leq 0.05$; ** $p \leq 0.01$; *** $p \leq 0.001$. Paired *t*-test: # $p \leq 0.05$. C/G: Paired *t*-test: * $p \leq 0.05$; ** $p \leq 0.01$. AU = arbitrary unit.

significant downregulation of IL-1b and NLRP3 gene expression in LPS-stimulated peritoneal cells by sHA (Fig. 1E). Transcriptional regulation of both IL-1b and NLRP3 following TLR signaling is dependent on NF κ B activation [57]. In previous studies we showed that sHA prevents phosphorylation of NF κ B and consequent transcription of NF κ B controlled pro-inflammatory genes [30–32]. The interference of IL-1b and NLRP3 gene expression suggests that sHA interrupts inflammasome activation on the level of TLR-mediated transcriptional priming of inflammasome components and downstream effector molecules [51].

In summary, our data reveal a direct immunoregulatory effect of sHA on murine macrophages and prove its high potential to reduce pro-inflammatory functions in these cells. This is consistent to our previous reports demonstrating anti-inflammatory effects on human macrophages and monocytes by solute sHA but also by collagen matrices containing sHA [30–32]. Mechanistically, sHA was taken up by the human macrophages via binding CD44 as well as the scavenger receptors CD36 and LOX-1 and induced the activation of anti-oxidative proteins. This interfered with TLR-induced activation of transcription factors like NF κ B, STAT1 and IRF5, resulting in reduced gene expression and release of pro-inflammatory cytokines including IL-1b, TNF, IL-12, IL-6, CCL2 in the macrophages [30]. Sulfated HA-mediated blockage of NF κ B and subsequent impaired release of pro-inflammatory factors like IL-6, IL-8, CCL2 and PGE2 was also reported in human mesenchymal stromal cells (MSC) [50]. This demonstrates that anti-inflammatory mechanisms of sHA also act on further cells with immune functions. Consistent to the findings in human macrophages and MSC we observed species-independent effects with reduced gene expression and release of pro-inflammatory cytokines in murine BM-derived and tissue-resident like peritoneal macrophages.

3.2. Modulation of pro-inflammatory macrophage functions by sulfated hyaluronan impairs inflammatory crosstalk of macrophages with skin cells

At wound sites, macrophages are in constant crosstalk with surrounding tissue cells and promote their activation and *vice versa* [58]. Epithelialization of wounds requires the activation of keratinocytes to proliferate and migrate over the wound bed. Although this includes macrophage-derived cytokines such as TNF, IL-1b, and IL-6 [59], excessive release of these factors under pathological conditions leads to deregulated keratinocyte differentiation and promotes their pro-inflammatory activation [45,60]. We therefore assessed whether the modulation of macrophage responses by sHA has an impact on the activation of keratinocytes using a skin *ex vivo* culture model, which allows the investigation of keratinocytes in a more physiological three-dimensional environment [61]. Interaction of macrophages with keratinocytes was mimicked by culture of skin biopsies from wild-type mice in supernatants from peritoneal cells as illustrated in Fig. 1F. Peritoneal cells were stimulated with either LPS alone or with sHA and subsequent LPS or were left unstimulated before supernatants were used for skin culture. To evaluate keratinocyte activation we analyzed epidermal expression of pro-inflammatory S100A9 and S100A8 that was shown to be up-regulated in a pathological crosstalk between macrophages and keratinocytes [45]. Culture of skin in supernatants of LPS

stimulated peritoneal cells resulted in a significant induction of S100A8 and S100A9 expression in the epidermis, while culture in supernatants of unstimulated peritoneal cells induced no activation of S100A8/A9 (Fig. 1G). Stimulation with LPS alone also induced no expression of S100A8/A9 in the cultured skin (Suppl. Fig. 2) indicating that factors derived from pro-inflammatory stimulated peritoneal cells mediate epidermal activation in the skin. Of note, supernatants from peritoneal cells treated with sHA before stimulation with LPS induced significantly less S100A8/9 expression in the epidermis (Fig. 1G). Stimulation procedure with sHA of peritoneal cells was slightly modified for skin *ex vivo* culture experiments to exclude any direct effect of sHA on the skin. Peritoneal cells were cultured with sHA for 24 h. Before the addition of LPS, cells were washed in order to generate sHA-free supernatants of stimulated peritoneal cells. In our previous study we had shown that anti-inflammatory activity of sHA on macrophages requires uptake of the GAG which occurs fast and within 24 h [30]. In line with this observation, pre-treatment for 24 h with sHA is efficient to effectively down-regulate inflammatory activation of peritoneal cells with reduced release of inflammatory factors in the supernatants used for skin culture (Suppl. Fig. 3). Although we do not untangle which macrophage-derived factors are responsible for epidermal activation in our *ex vivo* skin culture setting, our results indicate that compromised inflammatory activation of macrophages by sHA is effective to further impair the inflammatory crosstalk of macrophages with other skin cells.

3.3. Treatment with sulfated hyaluronan prevents and rescues skin inflammation in mice

Next, we analyzed the immunoregulatory impact of sHA on inflammatory processes in skin *in vivo*. Skin inflammation was induced in wild-type mice by topical application of the TLR7/8 agonist imiquimod (IMQ). First, we compared the regulatory effect of sHA with that of H-HA and L-HA. Different HA derivatives were injected in the IMQ-treated skin area at the same time with every IMQ application as illustrated in Fig. 2A. IMQ is a potent immune activator that induces a psoriasis-like dermatitis with inflamed and scaly skin lesions, epidermal thickening and massive immune cell infiltration [62]. Mice that were injected with sHA showed markedly less of these signs in the IMQ-treated skin. Redness and scaling of the skin was less pronounced in sHA-injected mice in comparison to mice injected with H-HA, L-HA or PBS (Fig. 2B). To further compare the inflammatory response in the skin we performed immunohistochemical analyses of hematoxylin/eosin (HE) stained skin tissue sections and visualized epidermal proliferation and immune cell infiltration by immunofluorescence (IF) stainings with the proliferation marker Ki67 and the myeloid cell marker CD11b, respectively. Epidermal thickening was significantly reduced in skin of sHA-treated mice in comparison to all other conditions (Fig. 2C). Consistently, activation of the proliferation marker Ki67 in the basal keratinocyte layer was significantly less in skin lesions treated with sHA (Fig. 2D). Furthermore, we observed a significantly reduced amount of infiltrated CD11b⁺ myeloid immune cells in the skin of sHA-treated mice (Fig. 2E). Further investigation revealed that reduced levels of CD11b⁺ cells are attributed to a reduction in F4/80⁺ macrophages in

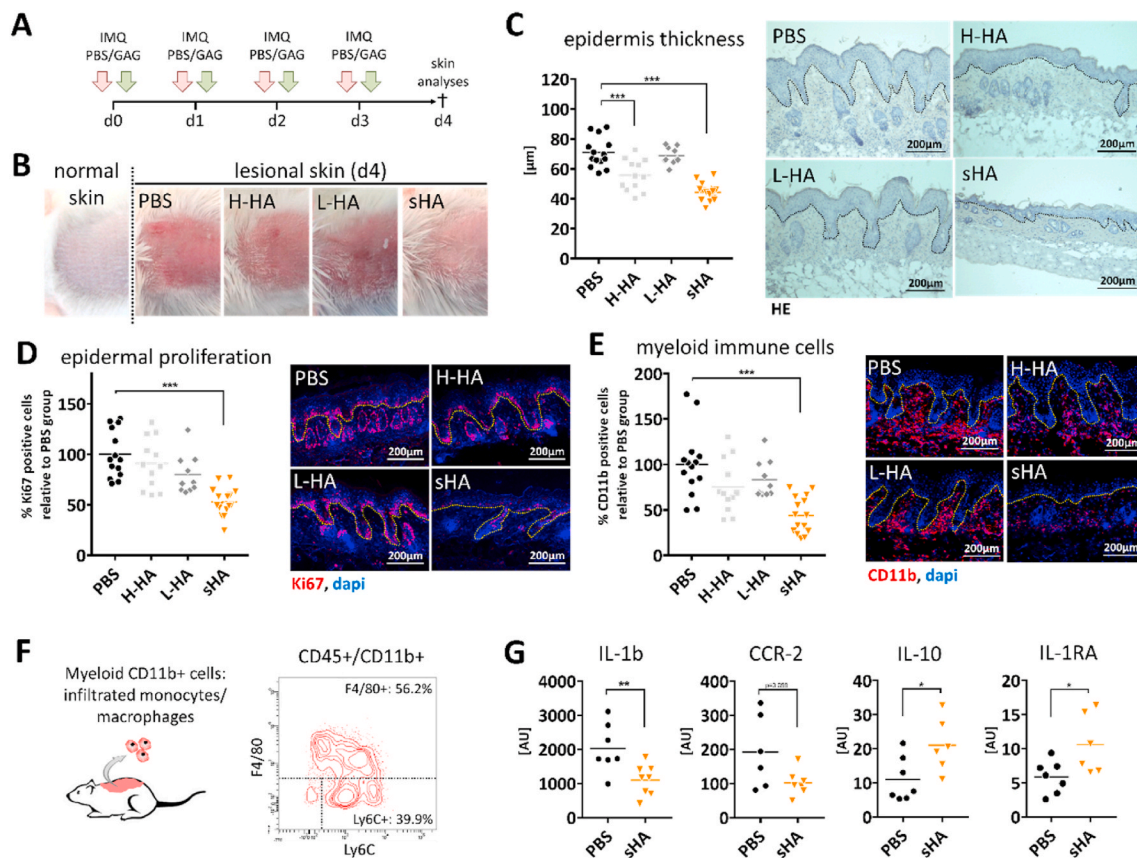


Fig. 2. Intradermal application of sHA attenuates IMQ-induced skin inflammation superior to native HA derivatives. Imiquimod (IMQ) was topically applied on the back skin of mice to induce an acute skin inflammation. At the same time either sulfated hyaluronan (sHA), high molecular weight HA (H-HA), low molecular weight HA (L-HA), or PBS was injected into skin. Skin inflammation was analyzed at day 4. **A)** Treatment regimen. **B)** Macroscopic appearance of lesional skin. **C)** Quantification of epidermis thickness and H&E staining of histological section of lesional skin. **D)** Quantification of Ki67 positive cells in the epidermis and immunofluorescence (IF) staining of Ki67 in lesional skin. **E)** Quantification of CD11b+ myeloid cells in lesional skin tissue and IF staining of CD11b+ in lesional skin sections. **F/G)** Analyses of CD11b+ myeloid cells isolated from lesional skin at day 3: **F)** Representative histogram of CD11b+ myeloid cells comprising F4/80+ macrophages and Ly6C+/F4/80- monocytes analyzed by flow cytometry. **G)** Gene expression relative to reference gene RS36B4 of pro-inflammatory (IL-1b/CCR2) and anti-inflammatory (IL-1RA/IL-10) markers in CD11b+ myeloid cells isolated from lesional skin. C–E: Dotted line marks border between epidermis and dermis. Each symbol represents one mouse. Line indicates mean. C–E: One-way ANOVA with multiple comparison to PBS: *** $p \leq 0.001$. G: Unpaired *t*-test: * $p \leq 0.05$; ** $p \leq 0.01$. AU = arbitrary unit.

the tissue, whereas the amount of PMN was unchanged (Suppl. Fig. 4). These results show a clear inhibitory effect of sHA on the inflammatory response in the skin compared to the native HA derivatives and support our observations from *in vitro* studies.

Next, we questioned whether reduced skin inflammation in sHA-treated mice is associated with a modulation of activated immune cells in the lesional skin. We treated mice simultaneously with IMQ and skin injections of either sHA or PBS (serving as control). At day 3, we isolated CD11b+ myeloid cells from the inflamed skin (Suppl. Fig. 5). As shown in Fig. 2F, majority (more than 95%) of the CD11b+ myeloid cells comprise Ly6C+/F4/80- cells and F4/80+ cells labeling infiltrated monocytes and macrophages, respectively. Lesional skin of IMQ-treated mice presents a strong inflammatory response with up-regulation of IL-1b and TNF (Suppl. Fig. 6) indicating a predominant pro-inflammatory immune cell activation in the skin at day 3. Indeed, gene expression analysis of CD11b+ cells isolated from lesional skin of PBS-treated mice showed high expression of the inflammatory markers IL-1b and CCR2, while the anti-inflammatory cytokines IL-10 and IL-1RA were only low expressed (Fig. 2G). Of note, expression of these factors was significantly changed in CD11b+ cells isolated from sHA-injected mice. The cells showed a downregulation of IL-1b and CCR2 in favor of an upregulation of IL-10 and IL-1RA (Fig. 2G). The chemokine receptor CCR2 marks Ly6C expressing monocytes that infiltrate from blood to injury sites in the early inflammatory phase and that differentiate to macrophages

with a pro-inflammatory role expressing pro-inflammatory cytokines including IL-1b [63,64]. Reduced expression of both CCR2 and IL-1b in isolated CD11b+ myeloid cells indicate a decreased proportion of pro-inflammatory activated cells in this population. Instead we found an upregulation of IL-10 and IL-1RA, two major cytokines for inflammatory resolution and typically produced by macrophages with an alternative M2-like activation [65]. This indicates a shift in macrophage activation towards resolution functions in the sHA-treated skin.

However, in our experimental design, we followed a prevention approach and applied sHA at the same time as inflammation was induced. To investigate whether sHA modulates the inflammatory response and macrophage activities of an established skin inflammation we changed our experimental setting from a prevention to a therapy approach. As depicted in Fig. 3A, we first applied IMQ on the back skin, after one day we injected sHA or PBS, and after 3 days we analyzed the inflammatory response in the lesional skin. At time of the first sHA injection, IMQ-treated skin presented a heavy pro-inflammatory response with infiltrated polymorphonuclear neutrophils (PMN) and monocytes/macrophages and the expression of inflammatory factors while anti-inflammatory mediators are downregulated (Suppl. Fig. 6). This shows that sHA treatment was started after the onset of inflammation. When we analyzed the mice at day 3, skin of mice injected with sHA appeared less inflamed as seen in the HE staining of histological skin sections (Fig. 3B) and showed reduced epidermal thickening (Fig. 3C) compared

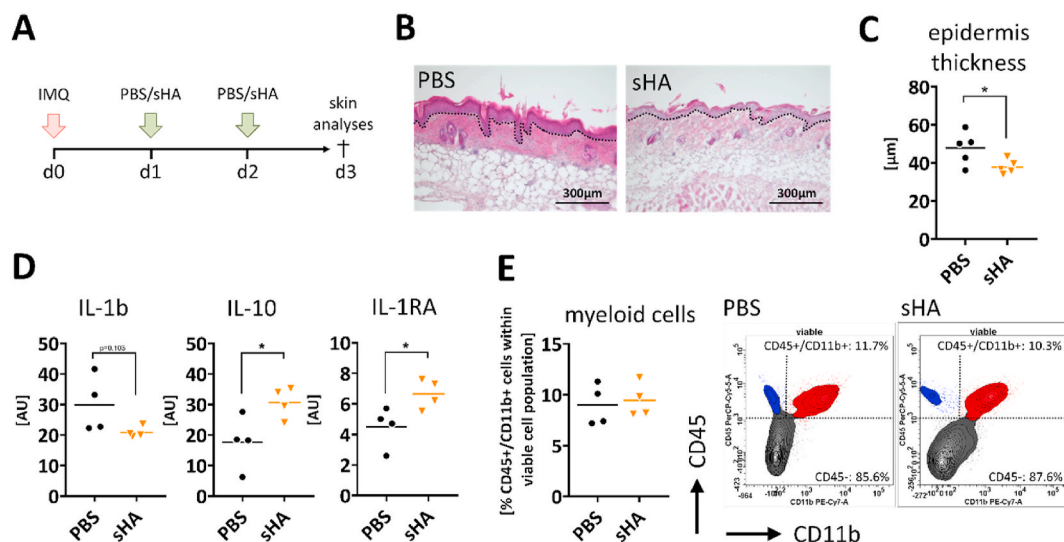


Fig. 3. Rescue of IMQ-induced skin inflammation by sHA is associated with a shift in macrophage activation towards anti-inflammatory functions. Acute skin inflammation was induced by topical application of one dose imiquimod on the back of mice. After one day sulfated hyaluronan (sHA) or PBS (control) were injected into the inflamed skin. Lesional skin was analyzed at day 3. **A)** Treatment regimen. **B)** H&E staining of histological sections of lesional skin. Dotted line marks border between epidermis and dermis. **C)** Quantification of epidermis thickness. **D)** Gene expression relative to reference gene RS36B4 of IL-1b, IL-1RA and IL-10 in CD11b + myeloid cells isolated from lesional skin. **E)** Infiltration of CD45+/CD11b + myeloid cells into lesional skin tissue determined by means of flow cytometry and representative histograms. Each symbol represents one mouse. Line indicates mean. Unpaired *t*-test: **p* ≤ 0.05; ***p* ≤ 0.01. AU = arbitrary unit.

to PBS injected mice. This demonstrates the ability of sHA to down-regulate established inflammation processes in the skin. Next, we isolated CD11b + myeloid cells comprising monocytes and macrophages from the inflamed skin (Suppl. Fig. 5). Gene expression analysis revealed a significant upregulation of the anti-inflammatory cytokines IL-10 and IL-1RA in isolated cells from sHA-treated mice while the inflammatory marker IL-1b is reduced (Fig. 3D). This analysis thus shows a similar result as the gene expression analysis of the isolated CD11b + cells from the prevention approach in Fig. 2. In contrast to the prevention approach where we applied sHA at the same time when inflammation was induced in the skin, infiltration of immune cells was not affected when sHA was injected after the onset of inflammation. As shown in Fig. 3E, we observed no differences in the level of infiltrated CD45+/CD11b+ myeloid cells in skin of PBS-treated and sHA-treated mice.

In summary, these data prove the anti-inflammatory activity of sHA *in vivo* by preventing and rescuing inflammation in the skin. Our *in vitro* experiments, demonstrating sHA-induced down-regulation of pro-inflammatory activities in macrophages, which further impair the inflammatory activation of skin cells, suggest similar mechanisms in the skin inflammation model. This is particularly supported by the results of the therapy approach, where sHA was injected after the onset of inflammation and no differences in the amount of infiltrated immune cells in the lesional skin of sHA-treated mice versus PBS-treated control mice was observed. This excludes the regulation of the inflammatory process via a modified infiltration of immune cells and indicates that reduced skin inflammation in sHA-treated skin predominantly results from a modulation of cells in the tissue by sHA.

In vitro experiments with murine macrophages in this study and with human macrophages in previous reports [30–32] have species-independently proved how sHA interferes with TLR-mediated activation of macrophages resulting in reduced expression of pro-inflammatory IL-1b, TNF, IL-12, CCL2 in favor of resolution markers like IL-10 and IL-1RA. Myeloid cells isolated from the sHA-treated skin in both approaches, prevention and therapy, mirror this activation profile in much aspects supporting our notion of sHA shifting macrophage activities from pro- to anti-inflammatory functions *in vivo*. Similar changes of macrophage phenotypes *in vivo* have been shown to reduce inflammation in other disease models. For example, application of immunoregulatory MSC and fibroblast in mouse models of peritonitis or

sepsis decreased TLR signaling in macrophages and promoted an alternative activation phenotype with elevated IL-10 activity [14,66,67].

In the prevention study we applied sHA at the same time as inflammation was induced suggesting an immediate effect of sHA in the tissue. In this treatment setting, we observed reduced levels of F4/80+ macrophages in the skin tissue of sHA-treated mice indicating an additional impact of sHA on immune cell infiltration. Macrophages differentiate from monocytes that infiltrate from the blood into inflamed sites under the control of chemokines like CCL-2 and CXCL-1 that are produced from resident cells in the injured area [68]. Reduced levels of macrophages may thus arise from reduced infiltration of monocytes into the lesional skin due to compromised chemokine activity in the tissue. We observed sHA-induced downregulation of CCL-2 and CXCL-1 in our *in vitro* experiments with tissue-resident like peritoneal cells (Fig. 1 A/C). This suggests a similar effect of sHA on skin resident macrophages resulting in reduced chemokines in the tissue. However, sulfated GAG also bind chemokines. Specifically, heparin derivatives were shown to bind pro-inflammatory chemokines such as CCL-2 and CXCL-1 and to neutralize their bioactivity on infiltrating PMN and monocytes [4]. Indeed, sHA was demonstrated to bind growth factors like transforming growth factor beta1 (TGFβ1) and vascular endothelial growth factor (VEGF) and to regulate the bioactivity of these factors on fibroblasts and endothelial cells [37,69,70]. Whether sHA also interacts with chemokines and controls their activity on immune cells was not investigated so far. We acknowledge that sHA may affect monocyte infiltration via such mechanism and may have contributed to the observed reduction of macrophages in lesional skin in the prevention approach.

Zhang et al. showed anti-inflammatory activities of sulfated semi-synthetic GAGs with HA-like structures in a murine model of rosacea and a model of croton oil induced dermatitis [71]. Mechanistically, semi-synthetic GAGs disrupt LL37 signaling, prevent RAGE-ligand interactions and thus reduce PMN infiltration and inflammation in the skin [71]. Interestingly, we observed no major effect on the level of infiltrated PMN in sHA-treated IMQ-skin neither in the prevention (Suppl. Fig. 4B) nor in the therapy approach (Suppl. Fig. 7) suggesting a possible interaction of sHA with LL37 and/or RAGE, although not investigated, to play no role in the sHA-mediated control of skin inflammation.

In summary, our data show a profound anti-inflammatory and immunoregulatory effect of sHA preventing and rescuing inflammation

in the skin via regulation of macrophage activation. This underlines the promising suitability of sHA as an immunomodulatory component for the control of inflammatory responses in the skin.

3.4. HA-AC/coll-based hydrogels continuously release sHA for up to 8 days

To transfer the immunomodulatory effect of sHA into wounds we adapted a previously published hydrogel system based on acrylated HA (HA-AC) and aECM [37]. The hydrogels are biocompatible and

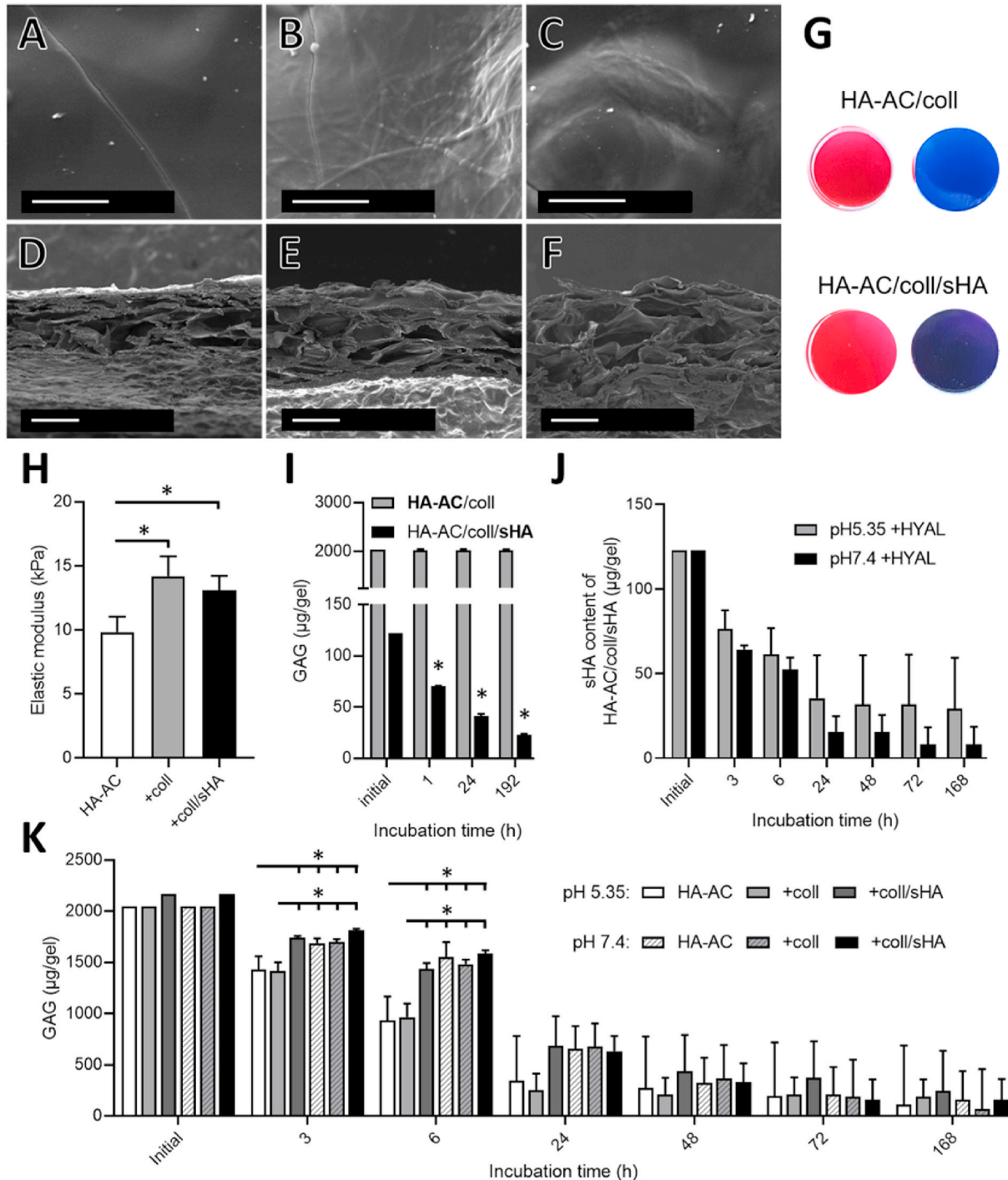


Fig. 4. Composition and elastic moduli of HA-AC/coll-based hydrogels. A-F) SEM images showing surface area (A–C) and morphology of cross-section (D–F). HA-AC without collagen (A/D), HA/coll (B/E) and HA/coll/sHA hydrogels (C/F). Scale bars: A-C 2 µm and D-F 50 µm. G) Staining for collagen and sHA with Sirius Red and Toluidine Blue, respectively. H) Elastic moduli as determined from the area with linear slope. Statistics: One-way ANOVA with *p < 0.05 considered significant. I) HA-AC (turbidity assay, light grey bar) or sHA (DMMB assay, black bar) remaining in hydrogels during incubation in PBS at 37 °C in comparison to the initially applied amounts. Statistics: One sample t-test against the initial sHA concentration with *p < 0.05 considered significant. J/K) Degradation of hydrogels at pH 5.35 or 7.4 with hyaluronidase (HYAL) at 37 °C. Remaining sHA (J) and total GAG amount (K) in hydrogels. One-way ANOVA with n = 4 for samples of the same time point with *p < 0.05 considered significant.

easy-to-manufacture. The production of HA-AC-based hydrogels is based on the use of photo-cross-linkable HA-AC, where fibrillar collagen matrices and GAG can be incorporated, thus enabling the hydrogel system to be adapted and modulated towards different applications. Here, we customized HA-AC-based hydrogels for the application in wounds and the release of sHA into the wound bed. We embedded sHA containing collagen-based aECM non-covalently in the HA-AC hydrogels (HA-AC/coll/sHA) and analyzed their mechanical properties and sHA release in comparison to blank HA-AC hydrogels (HA-AC) and HA-AC hydrogels embedded only with collagen-based aECM (HA-AC/coll).

SEM analysis of the hydrogels showed incorporation of aECM in the HA-AC scaffold with collagen containing HA-AC hydrogels displaying collagen fibrils at their surface (Fig. 4 B/C) in comparison to hydrogels made of HA-AC only displaying a smooth surface (Fig. 4A). Cross-sections of the hydrogels present a porous structure with pores of diverse pore dimensions (Fig. 4D–F). Furthermore, uniform staining by Sirius Red of both HA-AC/coll and HA-AC/coll/sHA hydrogels indicate that collagen is distributed uniformly in the hydrogels (Fig. 4G). Darker, violet color of HA-AC/coll/sHA hydrogels stained via Toluidine Blue compared to HA-AC/coll confirmed the presence and uniform distribution of sHA within the gels (Fig. 4G). The stress-strain curve of the 40 μ l cylinders displayed an almost linear slope in the range of 0.10 strain (Suppl. Fig. 8A). The elastic moduli of the analyzed hydrogels are slightly increased after incorporation of coll- and coll/sHA-based aECM, but with a range of 9.8–14.2 kPa (Fig. 4H) still similar to the Young's modulus of human skin (4.5–8 kPa) [72]. Softness and flexibility of the aECM containing hydrogels allows for their adaption to different wound shapes, making them suitable for use as wound dressings. In addition, porosity enables formation of a liquid phase between the moist hydrogels and the wound fluid facilitating the diffusion of released sHA from the hydrogel into the wounds.

Stability of the hydrogels and release of ECM components was analyzed in PBS at 37 °C over a period of 8 days. In line with our previous study [37], cross-linked HA-AC scaffolds remained stable during culture as seen by the release of less than 1% HA-AC from the HA-AC/coll hydrogels after 8 days determined by turbidity assay (Fig. 4I). Our analyses further showed that aECM-containing hydrogels released about two thirds of their non-covalently embedded collagen within the first hour of incubation in PBS, while at later time points almost no further collagen release was detectable (Suppl. Fig. 8B). This high initial boost release of collagen is attributed to the increased amount of collagen (1.5 mg/ml in this study compared to 0.5 mg/ml in Ref. [37]) that was used for the fabrication of the aECM-based HA-AC hydrogels. However, by increasing the initial sHA-concentration of the aECM-based HA-AC hydrogels, a substantial increase of the sHA amount was achieved, which was released from the hydrogels. After incubation over 8 days about 100 μ g sHA were detected in the supernatant as determined with the DMMB assay in Fig. 4I. This is a 5-time increased release of sHA from the HA-AC/coll/sHA hydrogels in comparison to the aECM-containing hydrogels in our previous study [37].

Since in the chronic wound milieu the hydrogels will be exposed to elevated levels of degrading enzymes like matrix metalloproteinases (MMPs) and HYAL [73,74] and the hydrogels are mainly composed of HA-AC, we performed HYAL degradation studies to reveal its influence on the stability of the hydrogels and the release of sHA. The HYAL degradation assay was performed analogously to a previous study at pH 7.4 [36] and, to obtain a more realistic degradation behavior analogous to the acidic milieu in the inflammatory wound healing phase, also at pH 5.35 [75].

The sHA content remaining in the hydrogels under degradation conditions over 168 h (7 d) did not differ significantly between the two pH conditions, although sHA release tended to be delayed at pH 5.35 (Fig. 4J). However, compared to HA-AC/coll/sHA hydrogels, incubated for 24 h in the absence of HYAL, the amount of sHA in the hydrogels was significantly smaller than after 24 h treatment with HYAL at pH 7.4

(Suppl. Fig. 8C) indicating that breakdown of the HA-AC hydrogel network accelerates the release of sHA.

With respect to the enzymatic hydrogel degradation as a whole, we observed a pH-dependent difference in the degradation of sHA-free hydrogels in the first 6 h of incubation (Fig. 4K). Within this time, degradation of these hydrogels at pH 5.35 is significantly faster than at pH 7.4 with a similar behavior of HA-AC hydrogels and HA-AC/coll hydrogels. HA/coll/sHA hydrogels, however, display a slower degradation rate at pH 5.35 in the first 6 h. In fact, degradation of the sHA containing hydrogel was similar at pH 5.35 and pH 7.4. This confirms previous findings that sHA can slow down digestion rate of HYAL [36]. For pH 7.4 no significant difference between the different hydrogels was detected at all time points. In contrast to the findings by Rother et al. the presence of fibrillar collagen did not appear to have an influence on enzymatic degradation [36]. This may be explained by the fact that higher concentration of HA-AC were used for the preparation of the hydrogels in the present study (5% w/w instead of 1% w/w in Ref. [36]) reducing the relative amount of collagen in the hydrogels and with this the impact of collagen on hydrogel degradation.

However, we stress out that the hydrogel degradation experiments were performed using a supraphysiological concentration of HYAL to simulate hydrogel stability and release of components under conditions of maximal degradation. Hence, hydrogels used under physiological HYAL concentrations *in vivo* may not degrade within the same time frame. In summary, sHA can be released from HA-AC/coll/sHA hydrogels in the absence of HYAL, but will have a continuous, sustained sHA release even during hydrogel degradation in the wound bed.

3.5. sHA-releasing HA-AC/coll-based hydrogels resolve inflammation and promote wound healing in diabetic db/db mice

We assessed the immunomodulatory capacity of sHA releasing HA-AC/coll hydrogels in skin wound healing of diabetic db/db mice that represents a relevant model for chronic wounds in human. Skin wounds of db/db mice replicate features of chronic wounds seen in patients with diabetes or chronic venous insufficiency (CVI) including delayed wound closure with impaired tissue formation and angiogenesis, unrestrained inflammation, and dysregulated macrophage activation [8–10]. Proving the sustained inflammatory response and defective M1/M2 shift as it is found in non-healing diabetic foot ulcers in patients [76], we observed in wounds of db/db mice increased expression of inflammatory genes including IL-1b, S100A9 and TNF while the expression of typical M2 macrophage markers like resistin-like molecule alpha (RELMA) and IL-10 [65] was decreased (Suppl. Fig. 9).

We treated full thickness excisional wounds with HA-AC/coll hydrogels or with HA-AC/coll/sHA hydrogels releasing sHA. To mimic a treatment situation in the patient, we applied the hydrogels 3 days after wounding when a substantial inflammation had developed in the wounds (Suppl. Fig. 10). In addition, we analyzed the effect of the hydrogels on the wounds at day 10 after wounding when the impaired wound healing phenotype in the diabetic db/db mice is fully developed in terms of increased inflammation, decreased M2 activation and delayed wound closure and the most resembles features of diabetic wound healing in patients. Treatment scheme of this therapeutic approach is depicted in Suppl. Fig. 11.

First, we analyzed the inflammatory response in the wound tissue. We observed reduced gene expression of inflammation markers IL-1b, S100A9, and NLRP3 in favor of an increased expression of RELMA, IL-10, and heme oxygenase 1 (HO-1) in wounds treated with sHA-releasing hydrogels compared to wounds treated with control HA-AC/coll hydrogels (Fig. 5A). This indicates a reduced inflammatory response in wounds of mice receiving HA-AC/coll/sHA hydrogels. Immunofluorescence (IF) staining of wound tissue with the macrophage marker F4/80 showed a similar amount of F4/80 positive macrophages in the wound tissue in both treatment groups (Fig. 5B). This was confirmed by F4/80 gene expression analysis of the wound tissue

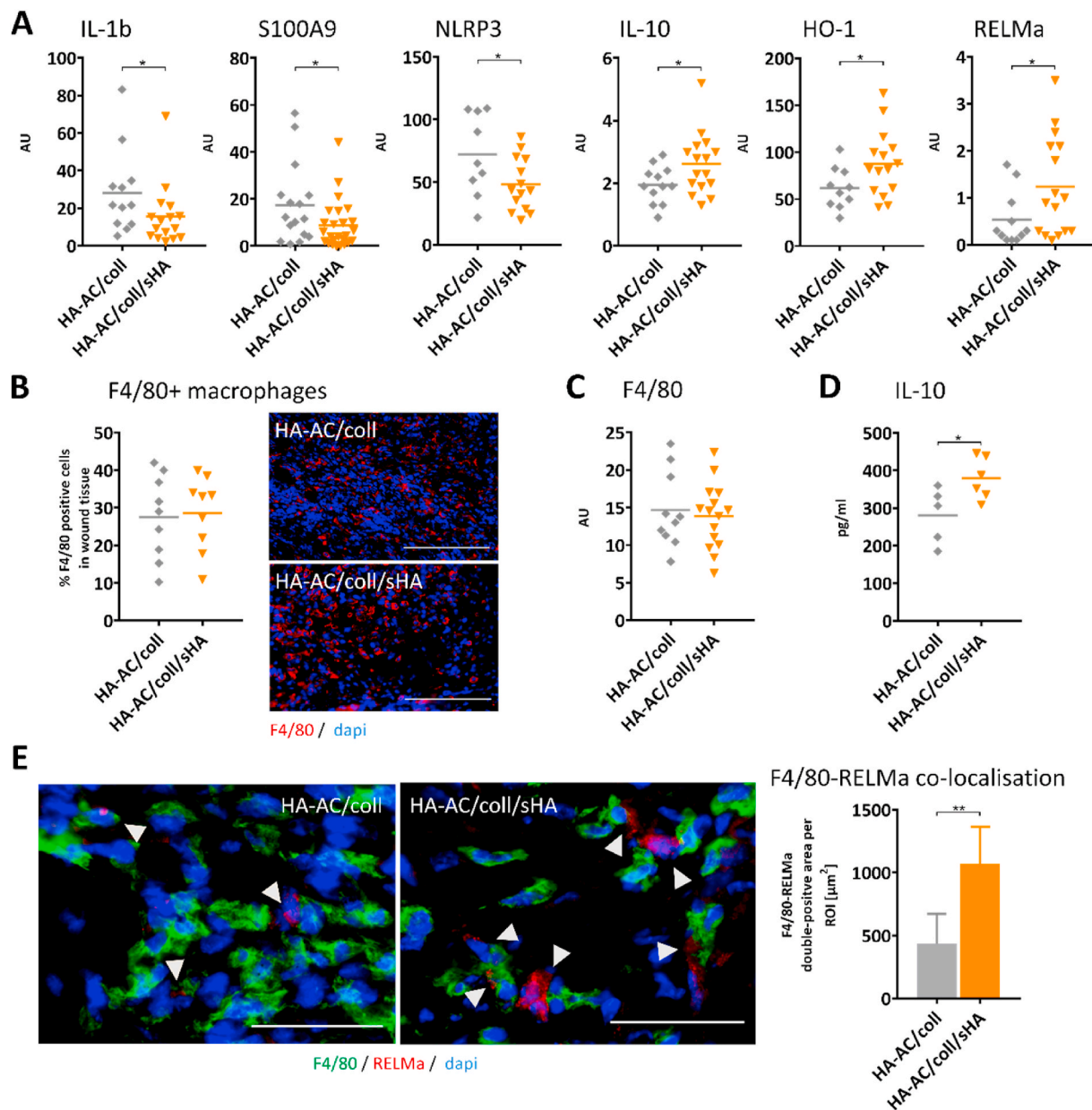


Fig. 5. Inflammation is reduced in favor of pro-regenerative macrophage functions in wounds of diabetic mice after treatment with sHA-releasing hydrogels. Wounds were inflicted by 6-mm punch biopsy on the backs of diabetic db/db mice. At day 3 post wounding control hydrogels (HA-AC/coll) or hydrogels containing sulfated hyaluronan (HA-AC/coll/sHA) were applied on the wounds. Wounds were analyzed 10 days post wounding. **A)** Gene expression relative to reference gene GAPDH of pro-inflammatory markers (IL-1b/S100A9/NLRP3) and pro-regenerative and anti-inflammatory macrophage markers (IL-10/HO-1/RELMa) in wound tissue. **B)** Quantification of F4/80+ macrophages in wound tissue and immunofluorescence (IF) staining of F4/80 visualizing macrophages in wound sections. Scale bar: 300 μ m **C)** F4/80 gene expression relative to reference gene GAPDH in wound tissue. **D)** Quantification of IL-10 protein in the wound tissue. **E)** IF staining of F4/80 and RELMa visualizing M2-like macrophages (double-positive, marked with arrow head) in wound sections and quantification of F4/80-RELMa co-localization. Granulation tissue was defined as region of interest (ROI). In each tissue section per mouse at least two areas of the same size within the ROI were analyzed. Mean \pm standard deviation. Scale bar: 50 μ m. B/D: Counterstaining DAPI (blue) for nuclei. Unpaired *t*-test: * $p \leq 0.05$; ** $p \leq 0.01$. AU = arbitrary unit.

(Fig. 5C). These data indicate that sHA releasing hydrogels – when applied on an existing inflammation - has no impact on the infiltration of immune cells paralleling our results from the skin inflammation study (Fig. 3). This suggests that the altered inflammatory process in wounds treated with HA-AC/coll/sHA hydrogels may result from a changed activation of macrophages in the wound tissue as it was observed in the skin inflammation model in Figs. 2G and 3D. This is supported by a study from Mirza et al., which shows sustained NLRP3 inflammasome activity and uncontrolled expression of IL-1b in wounds of diabetic db/db mice that derives from pro-inflammatory activated macrophages in the tissue

[10]. Consistent with this study we detected increased expression of NLRP3 and IL-1b in the wound tissue of our db/db mice. In wounds treated with HA-AC/coll/sHA hydrogels these factors are reduced suggesting that sHA released from the hydrogels interferes with the pro-inflammatory activation of macrophages in the wounds as shown in differentiated macrophages in Fig. 1D/E, and as observed in the acute skin inflammation model (Fig. 2G/3D). Mirza et al. further demonstrated, that blocking inflammasome activity and IL-1b in diabetic wounds induces healing-associated macrophage phenotypes expressing IL-10 [10,17]. Wounds treated with the HA-AC/coll/sHA hydrogels also

present upregulated expression of IL-10 and RELMa, a further characteristic pro-regenerative macrophage marker. This indicates that downregulation of pro-inflammatory functions like inflammasome and IL-1 by the sHA releasing hydrogels may induce a shift in macrophage activation states towards M2-like profiles in the wounds. This is further supported by the increased induction of anti-inflammatory HO-1 in these wounds. Expression of HO-1 in macrophages has been shown to promote their switch to an anti-inflammatory phenotype and to drive resolution of inflammatory responses [77,78].

To substantiate the observed induction of M2-like gene signatures in wounds after HA-AC/coll/sHA hydrogels treatment on protein level we quantified the production of IL-10 in the wound tissue. Consistent to the increased gene expression, we detected significantly more IL-10 protein in wounds treated with sHA releasing hydrogels (Fig. 5D). Next, we performed IF analyses in cryosections of wounds in which macrophages were double-stained with F4/80 and RELMa to visualize M2-like macrophages in the tissue. In wounds treated with sHA-releasing hydrogels (HA-AC/coll/sHA) we found more cells double positive for F4/80 and

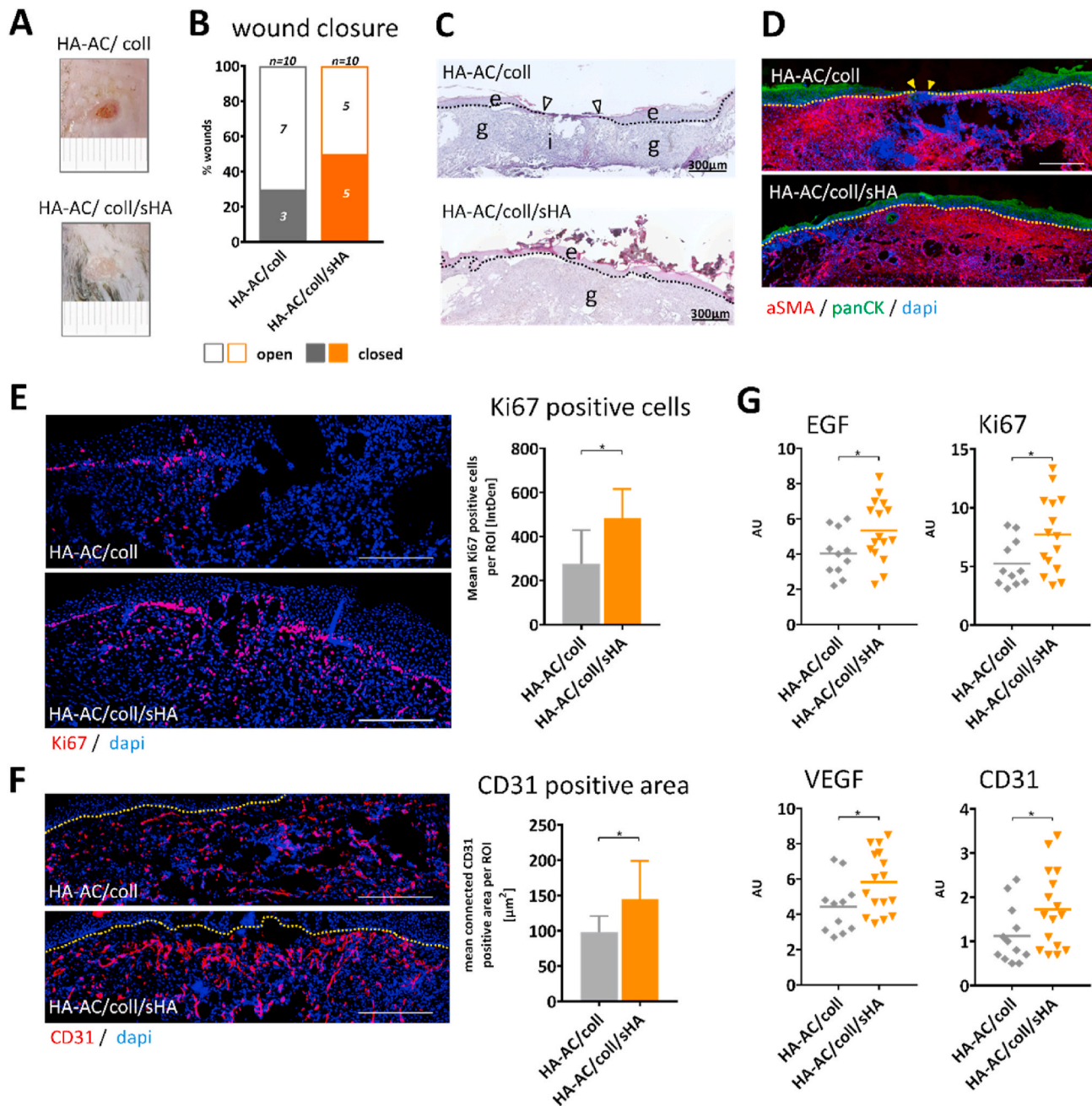


Fig. 6. Hydrogels releasing sHA accelerate re-epithelialization, tissue formation and angiogenesis in wounds in diabetic db/db mice. Wound study was performed as described in Fig. 5 and illustrated in Suppl. Fig. 11. **A)** Macroscopic appearance of wounds. **B)** Quantification of wound closure. **C)** H&E staining of wound sections. **D)** IF staining of aSMA and panCK in wound sections visualizing granulation tissue and neoepithelium, respectively. **E)** IF staining of Ki67 in wound sections visualizing proliferating cells and quantification of Ki67+ cells. Epidermal layer and granulation tissue were defined as region of interest (ROI). **F)** IF staining of CD31 in wound sections visualizing newly formed vessels and quantification of connected CD31+ area. Granulation tissue was defined as ROI. **G)** Gene expression relative to reference gene GAPDH of angiogenic markers (VEGF/CD31) and pro-regenerative tissue markers (EGF/Ki67) in wound tissue. g = granulation tissue; e = epidermis; i = immune cell infiltrate. Arrow head marks epithelial tip. Dotted line marks border between epidermis and dermis. Scale bars: 300 μ m. Each symbol represents one wound. Unpaired *t*-test: **p* \leq 0.05. AU = arbitrary unit. IntDen = integrated density.

RELMA than in wounds treated with the control hydrogels HA-AC/coll (Fig. 5E) demonstrating the increased activation of M2-like macrophages in these wounds.

In summary, reduced expression of IL-1b and NLRP3 together with the increased production of IL-10 and activation of RELMA in macrophages point to a modulation of macrophages towards pro-healing M2-like activation states in the wounds treated with sHA-releasing hydrogels.

Hence, wounds treated with HA-AC/coll/sHA hydrogels showed a faster closure (Fig. 6A) with half of the wounds (5 out of 10), while in the treatment cohort with control hydrogels (HA-AC/coll) only 3 out of 10 wounds had already closed (Fig. 6B). Immunohistochemical analyses of wound tissue sections were performed to visualize the tissue formation response. HE stainings present a closed neoepithelium and a fully developed granulation tissue with no remaining areas of immune cell infiltrates in most of the wounds treated with HA-AC/coll/sHA hydrogels (Fig. 6C). In addition, granulation tissue in these wounds is more mature containing a larger extent of alpha-smooth muscle actin (aSMA) positive cells and is covered by a fully developed cytokeratin (panCK) positive epidermal layer (Fig. 6D). Increased tissue formation is confirmed in IF analysis with the proliferation marker Ki67, which shows increased amounts of Ki67 positive cells in the wounds treated with HA-AC/coll/sHA hydrogels in comparison to those treated with the HA-AC/coll control hydrogels (Fig. 6E). IF-analysis of wound sections with the endothelial cell marker CD31 reveal an accelerated angiogenic response with advanced development of vascular structures in HA-AC/coll/sHA-treated wounds (Fig. 6F). We further performed gene expression analysis of tissue parameters and growth factors to substantiate the improved tissue response in wounds treated with sHA-releasing hydrogels (HA-AC/coll/sHA). First, we detect significantly elevated gene expression of Ki67 and CD31 in wounds treated with sHA-releasing hydrogels which is consistent with the increased activation of these factors in the wound tissue. Furthermore, gene expression of the epidermal growth factor (EGF) and of the pro-angiogenic factor VEGF is significantly increased in these wounds (Fig. 6G).

Particularly EGF and VEGF, but also the signaling molecule RELMA that is produced by M2-like macrophages in wounds and we found also up-regulated in HA-AC/coll/sHA-treated wounds (Fig. 5A/E) play an essential role in skin repair. Deficiency of these factors has been associated with chronic wounds and disturbed healing outcomes [11,79]. Increased expression of these pro-regenerative factors in the wound tissue after treatment with sHA-releasing hydrogels is reflected in the improved healing response of these wounds including accelerated wound closure, faster re-epithelialization, improved maturation of granulation tissue and increased vessel formation. M2-macrophage specific RELMA is involved in collagen assembly and important for the formation of functional granulation tissue [11], which is accelerated in the wounds with sHA-releasing hydrogels. EGF acts on epithelial cells and is crucial for the activation of keratinocyte migration and proliferation, thus contributing to re-epithelialization [80], which is increased in wounds treated with sHA-releasing HA-AC/coll/sHA hydrogels. In addition, EGF stimulates fibroblast proliferation and new tissue formation [81,82], which is also upregulated in these wounds and confirmed by the increase of Ki67 positive cells. VEGF is one of the most important pro-angiogenic factor in wound healing and induces the formation of new vascular structures in the wound tissue [83]. It acts as a mitogen and chemoattractant on CD31⁺ endothelial cells and induces vascular sprouting and outgrowth [84]. Wounds treated with HA-AC/coll/sHA hydrogels present an increased angiogenic response with more matured CD31 positive vessels and increased gene expression of CD31 in the wound tissue that is further substantiated by the increased expression of VEGF.

Due to its stimulating activity on skin cells both EGF and VEGF have been recognized as a promising agent for wound healing therapies [85]. Our sHA releasing hydrogels stimulate the activation of endogenous EGF and VEGF, which underlines their therapeutic potential. The

endogenous induction of EGF and VEGF indicates the formation of a pro-regenerative wound environment. The latter typically requires the activation of M2-like macrophage functions and resolution of inflammation [6] as we also observed in HA-AC/coll/sHA treated wounds. This fact together with the observed increase of M2-like markers suggests that sHA-releasing hydrogels induce their pro-regenerative activity on wounds via the shift of macrophage phenotypes involving the down-regulation of pro-inflammatory functions and the activation of pro-healing activities.

In addition to its direct immunoregulatory effect on cells, sHA also interacts with growth factors and may regulate cell functions indirectly by controlling their bioactivity. It was previously shown that sHA binds VEGF and reduces its angiogenic activity by blocking VEGF-mediated VEGF receptor-2 (VEGFR-2) signaling [70,86]. On the other hand, GAG also demonstrated to promote endothelial cell sprouting independent from VEGF [86]. Wounds treated with sHA releasing hydrogels show increased vessel formation and vascularization indicating no negative effect of sHA on the angiogenic response in the wound tissue. Interestingly, we have recently identified a novel mechanism by which sHA may control angiogenic processes in tissues involving its binding to VEGF, and to tissue inhibitor of metalloproteinase-3 (TIMP-3), an effective inhibitor of angiogenesis, that exerts its activity by competing with VEGF for binding to VEGFR-2 [69]. Binding of sHA blocks the interaction of both VEGF and TIMP3 with VEGFR-2. In a competitive setting binding of sHA to TIMP-3 partially rescues sHA-inhibited VEGF-A/VEGFR-2 signaling and endothelial cell activation.

Previously we reported on HA-AC/coll hydrogels containing sHA microgels as potential regulator of transforming growth factor-beta1 (TGF-b1) availability [37]. In wound healing, TGF-b1 is critically involved in fibroblast recruitment and activation and the formation of granulation tissue [87]. Inactivation of TGF-b1 function would thus compromise crucial steps of the wound healing response. In this study, we used HA-AC/coll/sHA hydrogels with a high release profile for sHA that present only low retention capacity of TGF-b1 suggesting low sequestration of TGFb-1 from the wound site. In line with this, we observed no negative effect on granulation tissue formation and TGF-b expression (data not shown). In contrast, regeneration was improved by sHA-releasing hydrogels, which suggests that the sHA-mediated regulation of immune cell activation overrides the negative influence of a possible binding of TGF-b1.

The use of bioactive materials in regenerative medicine is based on the idea of modifying signals in a respective wound microenvironment such that it facilitates healing and regeneration. Indeed, a variety of ECM-based materials for wound healing applications have been explored in recent years. Most of these materials focus on supporting tissue formation in wound healing by providing a scaffold for skin cell migration in wound tissue, by sustained delivery of growth factors that promote proliferation and activation of skin cells, or by being applied as a cell-colonized equivalent [88,89]. HA-based wound dressings have long been recognized for their pro-healing effects on skin wounds through hydrating the wounds and providing an environment favorable for migration and growth of skin cells including keratinocytes, fibroblasts and endothelial cells [90]. Hence, several commercially available HA-based wound dressings are used for management of acute and chronic wounds in the clinic. However, effectiveness of current chronic wound dressings is often unsatisfactory with slow progression in healing or no successful wound healing at all [2]. This requires new therapeutic approaches such as the control of unrestrained inflammatory processes in chronic wounds by immunomodulating wound dressings. Lohmann et al. developed an approach using GAG-based hydrogels to inactivate excessive pro-inflammatory chemokines in wound tissue, thereby reducing immune cell infiltration and, as a consequence, resolving inflammation and improving wound healing as they demonstrated in the same diabetic wound healing model in db/db mice as used in the present study [4]. Here, we present a novel immunomodulating approach for the control of inflammation in chronic wounds that is based on the

regulation of macrophages by HA/coll-based hydrogels releasing sHA as the active immunoregulatory compound for macrophage control. Macrophages have been recognized as main drivers of impaired healing in chronic wounds [9,10,91]. The concept of regulating macrophage activities in chronic wounds by an immunomodulating wound dressing is a very innovative approach and, to our knowledge, has not been explored before in this setting.

Our data show consistent anti-inflammatory activity of solute sHA on macrophages *in vitro* and *in vivo* and of hydrogel-released sHA on macrophages in wounds, which is independent from its molecular size. This is a particular advantage over the use of H-HA for macrophage modulation in chronic wounds. Chronic wounds of patients present increased activity of HYAL and higher levels of LMW-HA in comparison to acute healing wounds [73]. The accumulation of small HA fragments in chronic wounds reflects the inflammatory stress in the tissue [92] that may even be increased by the HA fragments when acting as a danger signal [93]. This demonstrates the risk of therapeutically applied H-HA to be degraded in chronic wounds that would most likely resolve its anti-inflammatory activity. It may also represent a limitation of HA-based wound dressings in clinical applications, although their anti-inflammatory effects and particularly the modulation of macrophage functions has not been investigated. In this respect, the use of sHA in immunomodulating hydrogels is a smart way to circumvent such undesired effects. In addition, sHA is hardly digested by HYAL and thus remains in its active form in the inflamed tissue [94].

Most of the currently used acellular ECM-based biomaterials for wound therapy are biodegradable scaffolds that provide their signals for wound modulation through disintegration at the wound site [95]. One advancement of our HA-AC/coll-based hydrogels is the integration of sHA as immunoregulatory component that is released from the hydrogel without material degradation. Release kinetic analyses show a prominent strong release of sHA within 24 h starting prompt after hydrogel contact with a liquid phase. However, we point out that our hydrogels are not protected from degradation and contain accessible target sites for MMPs and HYAL. Hydrogel degradation with HYAL increased sHA release and may accelerate the availability of sHA in the wound sites. After 7 days on the wounds of the db/db mice, hydrogels were still visible and not completely degraded, indicating rather slow degradation processes for the wound sites at least in mice. We therefore assume that sHA delivery from the hydrogels at the wound site consists of an initial release via diffusion, which may then be supplemented by an additional release from hydrogel degradation events.

In this respect, we acknowledge that in the course of a possible hydrogel degradation collagen and most prominently HA are also released in the wound environment and may modify the wound healing response. This may be reflected by the fact that wounds treated with HA-AC/coll-based hydrogels show faster closure in comparison to untreated wounds that were only covered by an inert non-bioactive, sterile wound dressing (Suppl. Fig. 12). This pro-healing effect of the HA-based HA-AC/coll hydrogels is consistent with reports on HA-based hydrogels that support wound healing by providing a moist environment and promoting cell migration [90]. Whether HA-AC/coll hydrogels promote wound healing by similar mechanisms remains to be investigated and is beyond the scope of this study. Increased closure of wounds after application of HA-AC/coll hydrogels in comparison to none-treated wounds demonstrates their suitability as HA-based control hydrogel. However, we acknowledge that the comparison with commercially available HA-based hydrogels would further substantiate the translational relevance of our findings. Nevertheless, HA-AC/coll/sHA hydrogels support wound healing in diabetic db/db mice superior to control HA-AC/coll hydrogels clearly showing that the delivery of sHA further improves the wound healing response. Our results show that the delivery of sHA has a particular modulating effect on inflammation and macrophage activities further facilitating and promoting the wound healing process. This points to the importance of sHA as immunoregulatory, pro-regenerative compound in our hydrogels.

4. Conclusion

Aim of this study was to investigate the suitability of sHA as immunoregulatory component in a hydrogel wound dressing for the modulation of dysregulated macrophage activities in chronic, non-healing wounds. Our findings demonstrate the downregulation of crucial pro-inflammatory macrophage activities in favor of the up-regulation of anti-inflammatory and pro-regenerative functions by sHA. This was found to be superior to native HA derivatives, and to have consequences for the activation of skin cells *in vitro* and in skin inflammation *in vivo*. Results from wound healing in db/db mice demonstrate the capability of sHA-releasing hydrogels to improve the outcome of disturbed skin wound healing by modulating macrophage activities contributing to continuous inflammation. In sum, our study confirms sHA as a potent immunoregulatory factor altering inflammation processes and suggests the application of sHA-based hydrogels as wound dressing material in the treatment of chronic, highly inflamed wounds. However, further analyses are required on the way to clinical translation, including refinement of the hydrogel manufacturing-process and choice of scaffold-components [95] as well as wound healing studies in animals with a skin physiology more closely resembling that of human skin [96].

CRedit authorship contribution statement

Sophia Hauck: Investigation, Formal analysis, Validation. **Paula Zager:** Investigation, Formal analysis, Validation. **Norbert Halfter:** Investigation, Formal analysis, Validation, Methodology, Visualization, Writing – review & editing. **Elke Wandel:** Investigation, Methodology. **Marta Torregrossa:** Investigation, Validation, Formal analysis. **Ainur Kakpenova:** Investigation, Validation, Formal analysis. **Sandra Rother:** Investigation, Formal analysis, Methodology, Visualization, Writing – original draft. **Michelle Ordieres:** Investigation. **Susann Räthel:** Investigation. **Albrecht Berg:** Investigation. **Stephanie Möller:** Investigation. **Matthias Schnabelrauch:** Funding acquisition, Resources, Writing – review & editing. **Jan C. Simon:** Conceptualization, Funding acquisition, Resources. **Vera Hintze:** Funding acquisition, Resources, Project administration, Supervision, Writing – review & editing. **Sandra Franz:** Funding acquisition, Resources, Project administration, Supervision, Conceptualization, Methodology, Visualization, Investigation, Formal analysis, Validation, Writing – original draft, Writing – review & editing.

Declaration of competing interest

The authors declare no conflict of interest.

Acknowledgments

This work was funded by the Deutsche Forschungsgemeinschaft (DFG, German Research Foundation) project number 59307082 – TRR67 subprojects A3, B3, Z3; project FR2671/4–1 to SF; project 420160411 to SR.

We thank Inka Forstreuter (University Leipzig) for excellent assistance in the *in vitro* and animal studies and Aline Katzschner (University Dresden) for vital help with the material preparation. V.H. acknowledges financial support by the TU Dresden “Zukunftskonzept” regarding the CellScale MicroTester, which was financed from funds of the excellence initiative of the federal and state governments of Germany.

Appendix A. Supplementary data

Supplementary data to this article can be found online at <https://doi.org/10.1016/j.bioactmat.2021.04.026>.

References

- [1] C.K. Sen, G.M. Gordillo, S. Roy, R. Kirsner, L. Lambert, T.K. Hunt, F. Gottrup, G. C. Gurtner, M.T. Longaker, Human skin wounds: a major and snowballing threat to public health and the economy, *Wound Repair Regen.* 17 (2009) 763–771, <https://doi.org/10.1111/j.1524-475X.2009.00543.x>.
- [2] G. Han, R. Ceilley, Chronic wound healing: a review of current management and treatments, *Adv. Ther.* 34 (2017) 599–610, <https://doi.org/10.1007/s12325-017-0478-y>.
- [3] S.A. Eming, M. Hammerschmidt, T. Krieg, A. Roers, Interrelation of immunity and tissue repair or regeneration, *Semin, Cell Dev. Biol.* 20 (2009) 517–527, <https://doi.org/10.1016/j.semcdb.2009.04.009>.
- [4] N. Lohmann, L. Schirmer, P. Atallah, E. Wandel, R.A. Ferrer, C. Werner, J.C. Simon, S. Franz, U. Freudenberg, Glycosaminoglycan-based hydrogels capture inflammatory chemokines and rescue defective wound healing in mice, *Sci. Transl. Med.* 9 (2017), <https://doi.org/10.1126/scitranslmed.aai9044>.
- [5] Z. Julier, A.J. Park, P.S. Briquez, M.M. Martino, Promoting tissue regeneration by modulating the immune system, *Acta Biomater.* 53 (2017) 13–28, <https://doi.org/10.1016/j.actbio.2017.01.056>.
- [6] T. Lucas, A. Waisman, R. Ranjan, J. Roes, T. Krieg, W. Müller, A. Roers, S.A. Eming, Differential roles of macrophages in diverse phases of skin repair, *J. Immunol.* 184 (2010) 3964–3977, <https://doi.org/10.4049/jimmunol.0903356>.
- [7] M.L. Novak, T.J. Koh, Phenotypic transitions of macrophages orchestrate tissue repair, *Am. J. Pathol.* 183 (2013) 1352–1363, <https://doi.org/10.1016/j.ajpath.2013.06.034>.
- [8] R. Mirza, T.J. Koh, Dysregulation of monocyte/macrophage phenotype in wounds of diabetic mice, *Cytokine* 56 (2011) 256–264, <https://doi.org/10.1016/j.cyt.2011.06.016>.
- [9] A. Sindrilari, T. Peters, S. Wieschalka, C. Baican, A. Baican, H. Peter, A. Hainzl, S. Schatz, Y. Qi, A. Schlecht, J.M. Weiss, M. Wlaschek, C. Sunderkötter, K. Scharffetter-Kochanek, An unrestrained proinflammatory M1 macrophage population induced by iron impairs wound healing in humans and mice, *J. Clin. Invest.* 121 (2011) 985–997, <https://doi.org/10.1172/JCI44490>.
- [10] R.E. Mirza, M.M. Fang, E.M. Weinheimer-Haus, W.J. Ennis, T.J. Koh, Sustained inflammasome activity in macrophages impairs wound healing in type 2 diabetic humans and mice, *Diabetes* 63 (2014) 1103–1114, <https://doi.org/10.2337/db13-0927>.
- [11] J.A. Knipper, S. Willenborg, J. Brinckmann, W. Bloch, T. Maaß, R. Wagener, T. Krieg, T. Sutherland, A. Munitz, M.E. Rothenberg, A. Niehoff, R. Richardson, M. Hammerschmidt, J.E. Allen, S.A. Eming, Interleukin-4 receptor α signaling in myeloid cells controls collagen fibril assembly in skin repair, *Immunity* 43 (2015) 803–816, <https://doi.org/10.1016/j.immuni.2015.09.005>.
- [12] P. Krzyszczyk, R. Schloss, A. Palmer, F. Berthiaume, The role of macrophages in acute and chronic wound healing and interventions to promote pro-wound healing phenotypes, *Front. Physiol.* 9 (2018) 419, <https://doi.org/10.3389/fphys.2018.00419>.
- [13] V. Falanga, S. Iwamoto, M. Chartier, T. Yufit, J. Butmarc, N. Koultab, D. Shryer, P. Carson, Autologous bone marrow-derived cultured mesenchymal stem cells delivered in a fibrin spray accelerate healing in murine and human cutaneous wounds, *Tissue Eng.* 13 (2007) 1299–1312, <https://doi.org/10.1089/ten.2006.0278>.
- [14] R.A. Ferrer, A. Saalbach, M. Grünwedel, N. Lohmann, I. Forstreuter, S. Saube, E. Wandel, J.C. Simon, S. Franz, Dermal fibroblasts promote alternative macrophage activation improving impaired wound healing, *J. Invest. Dermatol.* 137 (2017) 941–950, <https://doi.org/10.1016/j.jid.2016.11.035>.
- [15] Y. Qi, D. Jiang, A. Sindrilari, A. Stegemann, S. Schatz, N. Treiber, M. Rojewski, H. Schrezenmeier, S. Vander Beken, M. Wlaschek, M. Böhm, A. Seitz, N. Scholz, L. Hürselen, J. Brinckmann, A. Ignatius, K. Scharffetter-Kochanek, TSG-6 released from intradermally injected mesenchymal stem cells accelerates wound healing and reduces tissue fibrosis in murine full-thickness skin wounds, *J. Invest. Dermatol.* 134 (2014) 526–537, <https://doi.org/10.1038/jid.2013.328>.
- [16] Y. Wu, L. Chen, P.G. Scott, E.E. Tredget, Mesenchymal stem cells enhance wound healing through differentiation and angiogenesis, *Stem Cell.* 25 (2007) 2648–2659, <https://doi.org/10.1634/stemcells.2007-0226>.
- [17] R.E. Mirza, M.M. Fang, W.J. Ennis, T.J. Koh, Blocking interleukin-1 β induces a healing-associated wound macrophage phenotype and improves healing in type 2 diabetes, *Diabetes* 62 (2013) 2579–2587, <https://doi.org/10.2337/db12-1450>.
- [18] I. Goren, E. Müller, D. Schiefelbein, U. Christen, J. Pfeilschifter, H. Mühl, S. Frank, Systemic anti-TNF α treatment restores diabetes-impaired skin repair in ob/ob mice by inactivation of macrophages, *J. Invest. Dermatol.* 127 (2007) 2259–2267, <https://doi.org/10.1038/sj.jid.5700842>.
- [19] J.I. Andorko, C.M. Jewell, Designing biomaterials with immunomodulatory properties for tissue engineering and regenerative medicine, *Bioeng. Transl. Med.* 2 (2017) 139–155, <https://doi.org/10.1002/btm2.10063>.
- [20] S. Franz, S. Rammelt, D. Scharnweber, J.C. Simon, Immune responses to implants – a review of the implications for the design of immunomodulatory biomaterials, *Biomaterials* 32 (2011) 6692–6709, <https://doi.org/10.1016/j.biomaterials.2011.05.078>.
- [21] L.T. Saldin, M.C. Cramer, S.S. Velankar, L.J. White, S.F. Badylak, Extracellular matrix hydrogels from decellularized tissues: structure and function, *Acta Biomater.* 49 (2017) 1–15, <https://doi.org/10.1016/j.actbio.2016.11.068>.
- [22] J.L. Dziki, L. Huleihel, M.E. Scarritt, S.F. Badylak, Extracellular matrix bioscaffolds as immunomodulatory Biomaterials , *Tissue Eng.* 23 (2017) 1152–1159, <https://doi.org/10.1089/ten.TEA.2016.0538>.
- [23] R.O. Hynes, The extracellular matrix: not just pretty fibrils, *Science* 326 (2009) 1216–1219, <https://doi.org/10.1126/science.1176009>.
- [24] D. Jiang, J. Liang, J. Fan, S. Yu, S. Chen, Y. Luo, G.D. Prestwich, M. M. Mascarenhas, H.G. Garg, D.A. Quinn, R.J. Homer, D.R. Goldstein, R. Bucala, P. J. Lee, R. Medzhitov, P.W. Noble, Regulation of lung injury and repair by Toll-like receptors and hyaluronan, *Nat. Med.* 11 (2005) 1173–1179, <https://doi.org/10.1038/nm1315>.
- [25] A.J. Day, C.A. de La Motte, Hyaluronan cross-linking: a protective mechanism in inflammation? *Trends Immunol.* 26 (2005) 637–643, <https://doi.org/10.1016/j.it.2005.09.009>.
- [26] D. Krejcova, M. Pekarova, B. Safrankova, L. Kubala, The effect of different molecular weight hyaluronan on macrophage physiology, *Neuroendocrinol. Lett.* 30 (Suppl 1) (2009) 106–111.
- [27] J.E. Rayahin, J.S. Buhrman, Y. Zhang, T.J. Koh, R.A. Gemeinhart, High and low molecular weight hyaluronic acid differentially influence macrophage activation, *ACS Biomater. Sci. Eng.* 1 (2015) 481–493, <https://doi.org/10.1021/acsbiomaterials.5b00181>.
- [28] C.M. McKee, M.B. Penno, M. Cowman, M.D. Burdick, R.M. Strieter, C. Bao, P. W. Noble, Hyaluronan (HA) fragments induce chemokine gene expression in alveolar macrophages. The role of HA size and CD44, *J. Clin. Invest.* 98 (1996) 2403–2413.
- [29] P. Teder, R.W. Vandivier, D. Jiang, J. Liang, L. Cohn, E. Puré, P.M. Henson, P. W. Noble, Resolution of lung inflammation by CD44, *Science* 296 (2002) 155–158, <https://doi.org/10.1126/science.1069659>.
- [30] F. Jouy, N. Lohmann, E. Wandel, G. Ruiz-Gómez, M.T. Pisabarro, A.G. Beck-Sickinger, M. Schnabelrauch, S. Möller, J.C. Simon, S. Kalkhof, M. von Bergen, S. Franz, Sulfated hyaluronan attenuates inflammatory signaling pathways in macrophages involving induction of antioxidants, *Proteomics* 17 (2017), e1700082, <https://doi.org/10.1002/pmic.201700082>.
- [31] S. Franz, F. Allenstein, J. Kajahn, I. Forstreuter, V. Hintze, S. Möller, J.C. Simon, Artificial extracellular matrices composed of collagen I and high-sulfated hyaluronan promote phenotypic and functional modulation of human pro-inflammatory M1 macrophages, *Acta Biomater.* 9 (2013) 5621–5629, <https://doi.org/10.1016/j.actbio.2012.11.016>.
- [32] J. Kajahn, S. Franz, E. Rueckert, I. Forstreuter, V. Hintze, S. Moeller, J.C. Simon, Artificial extracellular matrices composed of collagen I and high sulfated hyaluronan modulate monocyte to macrophage differentiation under conditions of sterile inflammation, *Biomater* 2 (2012) 226–236, <https://doi.org/10.4161/biom.22855>.
- [33] V. Hintze, S. Moeller, M. Schnabelrauch, S. Bierbaum, M. Viola, H. Worch, D. Scharnweber, Modifications of hyaluronan influence the interaction with human bone morphogenetic protein-4 (hBMP-4), *Biomacromolecules* 10 (2009) 3290–3297, <https://doi.org/10.1021/bm9008827>.
- [34] J. Becher, S. Möller, M. Schnabelrauch, Phase transfer-catalyzed synthesis of highly acrylated hyaluronan, *Carbohydr. Polym.* 93 (2013) 438–441, <https://doi.org/10.1016/j.carbpol.2012.12.056>.
- [35] R. Kunze, M. Rösler, S. Möller, M. Schnabelrauch, T. Riemer, U. Hempel, P. Dieter, Sulfated hyaluronan derivatives reduce the proliferation rate of primary rat calvarial osteoblasts, *Glycoconj. J.* 27 (2010) 151–158, <https://doi.org/10.1007/s10719-009-9270-9>.
- [36] S. Rother, V.D. Galiazzo, D. Kilian, K.M. Fiebig, J. Becher, S. Moeller, U. Hempel, M. Schnabelrauch, J. Waltenberger, D. Scharnweber, V. Hintze, Hyaluronan/collagen hydrogels with sulfated hyaluronan for improved repair of vascularized tissue tune the binding of proteins and promote endothelial cell growth, *Macromol. Biosci.* 17 (2017), <https://doi.org/10.1002/mabi.201700154>.
- [37] S. Rother, V. Krönert, N. Hauck, A. Berg, S. Moeller, M. Schnabelrauch, J. Thiele, D. Scharnweber, V. Hintze, Hyaluronan/collagen hydrogel matrices containing high-sulfated hyaluronan microgels for regulating transforming growth factor- β 1, *J. Mater. Sci. Mater. Med.* 30 (2019) 65, <https://doi.org/10.1007/s10856-019-6267-1>.
- [38] S. Thönes, S. Rother, T. Wippold, J. Blaszkiewicz, K. Balamurugan, S. Moeller, G. Ruiz-Gómez, M. Schnabelrauch, D. Scharnweber, A. Saalbach, J. Rademann, M. T. Pisabarro, V. Hintze, U. Anderegg, Hyaluronan/collagen hydrogels containing sulfated hyaluronan improve wound healing by sustained release of heparin-binding EGF-like growth factor, *Acta Biomater.* 86 (2019) 135–147, <https://doi.org/10.1016/j.actbio.2019.01.029>.
- [39] B. Stadlinger, V. Hintze, S. Bierbaum, S. Möller, M.C. Schulz, R. Mai, E. Kuhlisch, S. Heinemann, D. Scharnweber, M. Schnabelrauch, U. Eckelt, Biological functionalization of dental implants with collagen and glycosaminoglycans – A comparative study, *J. Biomed. Mater. Res. B Appl. Biomater.* 100 (2012) 331–341, <https://doi.org/10.1002/jbm.b.31953>.
- [40] O.H. Lowry, N.J. Rosebrough, A.L. Farr, R.J. Randall, Protein measurement with the Folin phenol reagent, *J. Biol. Chem.* 193 (1951) 265–275.
- [41] R.W. Farndale, D.J. Buttle, A.J. Barrett, Improved quantitation and discrimination of sulphated glycosaminoglycans by use of dimethylmethylene blue, *Biochim. Biophys. Acta* 883 (1986) 173–177, [https://doi.org/10.1016/0304-4165\(86\)90306-5](https://doi.org/10.1016/0304-4165(86)90306-5).
- [42] J.-M. Song, J.-H. Im, J.-H. Kang, D.-J. Kang, A simple method for hyaluronic acid quantification in culture broth, *Carbohydr. Polym.* 78 (2009) 633–634, <https://doi.org/10.1016/j.carbpol.2009.04.033>.
- [43] S. Rother, J. Saalbach-Hirsch, S. Moeller, T. Seemann, M. Schnabelrauch, L. C. Hofbauer, V. Hintze, D. Scharnweber, Bioinspired collagen/glycosaminoglycan-based cellular microenvironments for tuning osteoclastogenesis, *ACS Appl. Mater. Interfaces* 7 (2015) 23787–23797, <https://doi.org/10.1021/acsami.5b08419>.
- [44] E.A. Balazs, K.O. Berntsen, J. Karossa, D.A. Swann, An automated method for the determination of hexosamines, *Nat. Biochem.* 12 (1965) 559–564, [https://doi.org/10.1016/0003-2697\(65\)90222-8](https://doi.org/10.1016/0003-2697(65)90222-8).

- [45] D. Herbert, S. Franz, Y. Popkova, U. Anderegg, J. Schiller, K. Schwede, A. Lorz, J. C. Simon, A. Saalbach, High-fat diet exacerbates early psoriatic skin inflammation independent of obesity: saturated fatty acids as key players, *J. Invest. Dermatol.* 138 (2018) 1999–2009, <https://doi.org/10.1016/j.jid.2018.03.1522>.
- [46] K. Stelzner, D. Herbert, Y. Popkova, A. Lorz, J. Schiller, M. Gericke, N. Klötting, M. Blüher, S. Franz, J.C. Simon, A. Saalbach, Free fatty acids sensitize dendritic cells to amplify TH1/TH17-immune responses, *Eur. J. Immunol.* 46 (2016) 2043–2053, <https://doi.org/10.1002/eji.201546263>.
- [47] T.A. Wynn, K.M. Vannella, Macrophages in tissue repair, regeneration, and fibrosis, *Immunity* 44 (2016) 450–462, <https://doi.org/10.1016/j.immuni.2016.02.015>.
- [48] S.A. Eming, P. Martin, M. Tomic-Canic, Wound repair and regeneration: mechanisms, signaling, and translation, *Sci. Transl. Med.* 6 (2014) 265sr6, <https://doi.org/10.1126/scitranslmed.3009337>.
- [49] Y. Okabe, Molecular control of the identity of tissue-resident macrophages, *Int. Immunol.* 30 (2018) 485–491, <https://doi.org/10.1093/intimm/dxy019>.
- [50] U. Hempel, C. Matthäus, C. Preissler, S. Möller, V. Hintze, P. Dieter, Artificial matrices with high-sulfated glycosaminoglycans and collagen are anti-inflammatory and pro-osteogenic for human mesenchymal stromal cells, *J. Cell. Biochem.* 115 (2014) 1561–1571, <https://doi.org/10.1002/jcb.24814>.
- [51] S. Christgen, D.E. Place, T.-D. Kanneganti, Toward targeting inflammasomes: insights into their regulation and activation, *Cell Res.* 30 (2020) 315–327, <https://doi.org/10.1038/s41422-020-0295-8>.
- [52] N. Kelley, D. Jeltema, Y. Duan, Y. He, The NLRP3 inflammasome: an overview of mechanisms of activation and regulation, *Int. J. Mol. Sci.* 20 (2019), <https://doi.org/10.3390/ijms20133328>.
- [53] S. Legrand-Poels, N. Esser, L. L'homme, A. Scheen, N. Paquot, J. Piette, Free fatty acids as modulators of the NLRP3 inflammasome in obesity/type 2 diabetes, *Biochem. Pharmacol.* 92 (2014) 131–141, <https://doi.org/10.1016/j.bcp.2014.08.013>.
- [54] M.A. Gianfrancesco, J. Dehairs, L. L'homme, G. Herinckx, N. Esser, O. Jansen, Y. Habraken, C. Lassence, J.V. Swinnen, M.H. Rider, J. Piette, N. Paquot, S. Legrand-Poels, Saturated fatty acids induce NLRP3 activation in human macrophages through K⁺ efflux resulting from phospholipid saturation and Na, K-ATPase disruption, *Biochim. Biophys. Acta Mol. Cell Biol. Lipids* 1864 (2019) 1017–1030, <https://doi.org/10.1016/j.bbalip.2019.04.001>.
- [55] M.M. Robblee, C.C. Kim, J. Porter Abate, M. Valdearcos, K.L.M. Sandlund, M. K. Shenoy, R. Volmer, T. Iwawaki, S.K. Koliwad, Saturated fatty acids engage an IRE1 α -dependent pathway to activate the NLRP3 inflammasome in myeloid cells, *Cell Rep.* 14 (2016) 2611–2623, <https://doi.org/10.1016/j.celrep.2016.02.053>.
- [56] G.J. van der Vusse, Albumin as fatty acid transporter, *Drug Metabol. Pharmacokinet.* 24 (2009) 300–307, <https://doi.org/10.2133/dmpk.24.300>.
- [57] F.G. Bauernfeind, G. Horvath, A. Stutz, E.S. Alnemri, K. MacDonald, D. Speert, T. Fernandes-Alnemri, J. Wu, B.G. Monks, K.A. Fitzgerald, V. Hornung, E. Latz, Cutting edge: NF- κ B activating pattern recognition and cytokine receptors license NLRP3 inflammasome activation by regulating NLRP3 expression, *J. Immunol.* 183 (2009) 787–791, <https://doi.org/10.4049/jimmunol.0901363>.
- [58] J.C. Brazil, M. Quiros, A. Nusrat, C.A. Parkos, Innate immune cell-epithelial crosstalk during wound repair, *J. Clin. Invest.* 129 (2019) 2983–2993, <https://doi.org/10.1172/JCI124618>.
- [59] T. Xiao, Z. Yan, S. Xiao, Y. Xia, Proinflammatory cytokines regulate epidermal stem cells in wound epithelialization, *Stem Cell Res. Ther.* 11 (2020) 232, <https://doi.org/10.1186/s13287-020-01755-y>.
- [60] M.L. Usui, J.N. Mansbridge, W.G. Carter, M. Fujita, J.E. Olerud, Keratinocyte migration, proliferation, and differentiation in chronic ulcers from patients with diabetes and normal wounds, *J. Histochem. Cytochem.* 56 (2008) 687–696, <https://doi.org/10.1369/jhc.2008.951194>.
- [61] B.M. Baker, C.S. Chen, Deconstructing the third dimension – how 3D culture microenvironments alter cellular cues, *J. Cell Sci.* 125 (2012) 3015–3024, <https://doi.org/10.1242/jcs.079509>.
- [62] L. van der Fits, S. Mourits, J.S.A. Voerman, M. Kant, L. Boon, J.D. Laman, F. Cornelissen, A.-M. Mus, E. Florencia, E.P. Prens, E. Lubberts, Imiquimod-induced psoriasis-like skin inflammation in mice is mediated via the IL-23/IL-17 axis, *J. Immunol.* 182 (2009) 5836–5845, <https://doi.org/10.4049/jimmunol.0802999>.
- [63] D. Dal-Secco, J. Wang, Z. Zeng, E. Kolaczowska, C.H.Y. Wong, B. Petri, R. M. Ransohoff, I.F. Charo, C.N. Jenne, P. Kubas, A dynamic spectrum of monocytes arising from the in situ reprogramming of CCR2⁺ monocytes at a site of sterile injury, *J. Exp. Med.* 212 (2015) 447–456, <https://doi.org/10.1084/jem.20141539>.
- [64] A.E. Boniakowski, A.S. Kimball, A. Joshi, M. Schaller, F.M. Davis, A. denDekker, A. T. Obi, B.B. Moore, S.L. Kunkel, K.A. Gallagher, Macrophage chemokine receptor CCR2 plays a crucial role in macrophage recruitment and regulated inflammation in wound healing, *Eur. J. Immunol.* 48 (2018) 1445–1455, <https://doi.org/10.1002/eji.201747400>.
- [65] F.O. Martinez, S. Gordon, The M1 and M2 paradigm of macrophage activation: time for reassessment, *F1000Prime Rep.* 6 (2014) 13, <https://doi.org/10.12703/P6-13>.
- [66] H. Choi, R.H. Lee, N. Bazhanov, J.Y. Oh, D.J. Prockop, Anti-inflammatory protein TSG-6 secreted by activated MSCs attenuates zymosan-induced mouse peritonitis by decreasing TLR2/NF- κ B signaling in resident macrophages, *Blood* 118 (2011) 330–338, <https://doi.org/10.1182/blood-2010-12-327353>.
- [67] K. Németh, A. Leelahavanichkul, P.S.T. Yuen, B. Mayer, A. Parmelee, K. Doi, P. G. Robey, K. Leelahavanichkul, B.H. Koller, J.M. Brown, X. Hu, I. Jelinek, R.A. Star, E. Mezey, Bone marrow stromal cells attenuate sepsis via prostaglandin E(2)-dependent reprogramming of host macrophages to increase their interleukin-10 production, *Nat. Med.* 15 (2009) 42–49, <https://doi.org/10.1038/nm.1905>.
- [68] B. Moser, K. Willmann, Chemokines: role in inflammation and immune surveillance, *Ann. Rheum. Dis.* 63 (Suppl 2) (2004) ii84–ii89, <https://doi.org/10.1136/ard.2004.028316>.
- [69] S. Rother, S.A. Samsonov, S. Moeller, M. Schnabelrauch, J. Rademann, J. Blaszkiewicz, S. Köhling, J. Waltenberger, M.T. Pisabarro, D. Scharnweber, V. Hintze, Sulfated hyaluronan alters endothelial cell activation in vitro by controlling the biological activity of the angiogenic factors vascular endothelial growth factor-A and tissue inhibitor of metalloproteinase-3, *ACS Appl. Mater. Interfaces* 9 (2017) 9539–9550, <https://doi.org/10.1021/acsmi.7b01300>.
- [70] D.-K. Lim, R.G. Wylie, R. Langer, D.S. Kohane, Selective binding of C-6 OH sulfated hyaluronic acid to the angiogenic isoform of VEGF(165), *Biomaterials* 77 (2016) 130–138, <https://doi.org/10.1016/j.biomaterials.2015.10.074>.
- [71] J. Zhang, X. Xu, N.V. Rao, B. Argyle, L. McCoard, W.J. Rusho, T.P. Kennedy, G. D. Prestwich, G. Krueger, Novel sulfated polysaccharides disrupt cathelicidins, inhibit RAGE and reduce cutaneous inflammation in a mouse model of rosacea, *PLoS One* 6 (2011), e16658, <https://doi.org/10.1371/journal.pone.0016658>.
- [72] C. Pailler-Mattei, S. Bec, H. Zahouani, In vivo measurements of the elastic mechanical properties of human skin by indentation tests, *Med. Eng. Phys.* 30 (2008) 599–606, <https://doi.org/10.1016/j.medengphy.2007.06.011>.
- [73] T.A. Dechert, A.E. Ducale, S.I. Ward, D.R. Yager, Hyaluronan in human acute and chronic dermal wounds, *Wound Repair Regen.* 14 (2006) 252–258, <https://doi.org/10.1111/j.1743-6109.2006.00119.x>.
- [74] J.L. Lazaro, V. Izzo, S. Meaume, A.H. Davies, R. Lobmann, L. Uccioli, Elevated levels of matrix metalloproteinases and chronic wound healing: an updated review of clinical evidence, *J. Wound Care* 25 (2016) 277–287, <https://doi.org/10.12968/jowc.2016.25.5.277>.
- [75] L.A. Schneider, A. Korber, S. Grabbe, J. Dissemmond, Influence of pH on wound-healing: a new perspective for wound-therapy? *Arch. Dermatol. Res.* 298 (2007) 413–420, <https://doi.org/10.1007/s00403-006-0713-x>.
- [76] S. Nassiri, I. Zakeri, M.S. Weingarten, K.L. Spiller, Relative expression of proinflammatory and antiinflammatory genes reveals differences between healing and nonhealing human chronic diabetic foot ulcers, *J. Invest. Dermatol.* 135 (2015) 1700–1703, <https://doi.org/10.1038/jid.2015.30>.
- [77] Y. Naito, T. Takagi, Y. Higashimura, Heme oxygenase-1 and anti-inflammatory M2 macrophages, *Arch. Biochem. Biophys.* 564 (2014) 83–88, <https://doi.org/10.1016/j.abb.2014.09.005>.
- [78] V. Vijayan, F.A.D.T.G. Wagener, S. Immenschuh, The macrophage heme-heme oxygenase-1 system and its role in inflammation, *Biochem. Pharmacol.* 153 (2018) 159–167, <https://doi.org/10.1016/j.bcp.2018.02.010>.
- [79] S. Barrientos, H. Brem, O. Stojadinovic, M. Tomic-Canic, Clinical application of growth factors and cytokines in wound healing, *Wound Repair Regen.* 22 (2014) 569–578, <https://doi.org/10.1111/wrr.12205>.
- [80] I. Haase, R. Evans, R. Pofahl, F.M. Watt, Regulation of keratinocyte shape, migration and wound epithelialization by IGF-1- and EGF-dependent signalling pathways, *J. Cell Sci.* 116 (2003) 3227–3238, <https://doi.org/10.1242/jcs.00610>.
- [81] K.J. Lembach, Induction of human fibroblast proliferation by epidermal growth factor (EGF): enhancement by an EGF-binding arginine esterase and by ascorbate, *Proc. Natl. Acad. Sci. U.S.A.* 73 (1976) 183–187, <https://doi.org/10.1073/pnas.73.1.183>.
- [82] D. Kim, S.Y. Kim, S.K. Mun, S. Rhee, B.J. Kim, Epidermal growth factor improves the migration and contractility of aged fibroblasts cultured on 3D collagen matrices, *Int. J. Mol. Med.* 35 (2015) 1017–1025, <https://doi.org/10.3892/ijmm.2015.2088>.
- [83] N.N. Nissen, P.J. Polverini, A.E. Koch, M.V. Volin, R.L. Gamelli, L.A. DiPietro, Vascular endothelial growth factor mediates angiogenic activity during the proliferative phase of wound healing, *Am. J. Pathol.* 152 (1998) 1445–1452.
- [84] K.E. Johnson, T.A. Wilgus, Vascular endothelial growth factor and angiogenesis in the regulation of cutaneous wound repair, *Adv. Wound Care* 3 (2014) 647–661, <https://doi.org/10.1089/wound.2013.0517>.
- [85] H. Kim, W.H. Kong, K.-Y. Seong, D.K. Sung, H. Jeong, J.K. Kim, S.Y. Yang, S. K. Hahn, Hyaluronate-epidermal growth factor conjugate for skin wound healing and regeneration, *Biomacromolecules* 17 (2016) 3694–3705, <https://doi.org/10.1021/acs.biomac.6b01216>.
- [86] L. Koehler, G. Ruiz-Gómez, K. Balamurugan, S. Rother, J. Freyse, S. Möller, M. Schnabelrauch, S. Köhling, S. Djordjevic, D. Scharnweber, J. Rademann, M. T. Pisabarro, V. Hintze, Dual action of sulfated hyaluronan on angiogenic processes in relation to vascular endothelial growth factor-A, *Sci. Rep.* 9 (2019) 18143, <https://doi.org/10.1038/s41598-019-54211-0>.
- [87] R.W.D. Gilbert, M.K. Vickaryous, A.M. Vitoria-Petit, Signalling by transforming growth factor beta isoforms in wound healing and tissue regeneration, *J. Dev. Biol.* 4 (2016), <https://doi.org/10.3390/jdb4020021>.
- [88] H. Sodhi, A. Panitch, Glycosaminoglycans in tissue engineering: a review, *Biomolecules* 11 (2020), <https://doi.org/10.3390/biom11010029>.
- [89] T. Walimbe, A. Panitch, Proteoglycans in biomedicine: resurgence of an underexploited class of ECM molecules, *Front. Pharmacol.* 10 (2019) 1661, <https://doi.org/10.3389/fphar.2019.01661>.
- [90] M.F.P. Graça, S.P. Miguel, C.S.D. Cabral, I.J. Correia, Hyaluronic acid-Based wound dressings: a review, *Carbohydr. Polym.* 241 (2020) 116364, <https://doi.org/10.1016/j.carbpol.2020.116364>.
- [91] R.E. Mirza, M.M. Fang, M.L. Novak, N. Urao, A. Sui, W.J. Ennis, T.J. Koh, Macrophage PPAR γ and impaired wound healing in type 2 diabetes, *J. Pathol.* 236 (2015) 433–444, <https://doi.org/10.1002/path.4548>.
- [92] K.L. Aya, R. Stern, Hyaluronan in wound healing: rediscovering a major player, *Wound Repair Regen.* 22 (2014) 579–593, <https://doi.org/10.1111/wrr.12214>.
- [93] J.D. Powell, M.R. Horton, Threat matrix: low-molecular-weight hyaluronan (HA) as a danger signal, *IR* 31 (2005) 207–218, <https://doi.org/10.1385/IR:31:3:207>.

- [94] K. Lemmnitzer, J. Schiller, J. Becher, S. Möller, M. Schnabelrauch, Improvement of the digestibility of sulfated hyaluronans by bovine testicular hyaluronidase: a UV spectroscopic and mass spectrometric study, *BioMed Res. Int.* 2014 (2014) 986594, <https://doi.org/10.1155/2014/986594>.
- [95] N.J. Turner, S.F. Badylak, The use of biologic scaffolds in the treatment of chronic nonhealing wounds, *Adv. Wound Care* 4 (2015) 490–500, <https://doi.org/10.1089/wound.2014.0604>.
- [96] M. Seaton, A. Hocking, N.S. Gibran, Porcine models of cutaneous wound healing, *ILAR J.* 56 (2015) 127–138, <https://doi.org/10.1093/ilar/ilv016>.